AD-A094 659 NAVAL RESEARCH LAB WASHINGTON DC F/G 20/6
OCEAN ENVIRONMENTAL INFLUENCES OF TEMPERATURE AND MECHANICAL ST--ETC(U)
JAN 81 S HANISH
UNCLASSIFIED NRL-8424 NL

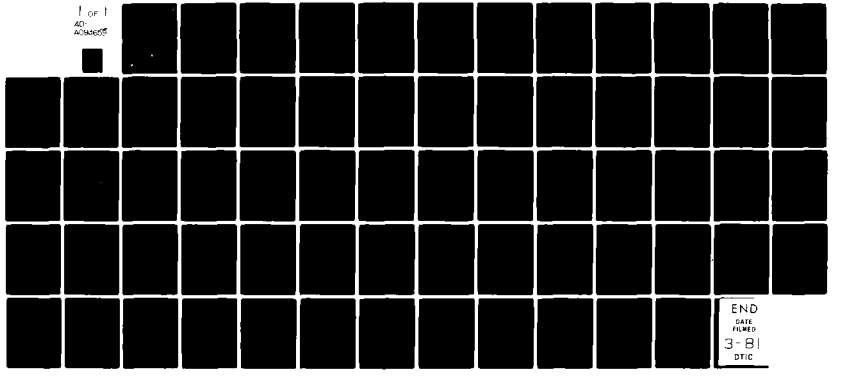

NRL Report 8424

Ocean Environmental Influences of Temperature and Mechanical Stress on Bare Fiber-Optic Sensors of Acoustic Pressures
Part I

S. HANISH

Acoustics Division

January 6, 1981

NAVAL RESEARCH LABORATORY
Washington, D.C.

(9) Final Rept.

SECURITY CLASSIFICATION OF THIS PAGE (When Data Entered)

REPORT DOCUMENTATION PAGE

READ INSTRUCTIONS BEFORE COMPLETING FORM

(14) 1. REPORT NUMBER: NRL Report 8424

2. GOVT ACCESSION NO.: AD-A094 659

3. RECIPIENT'S CATALOG NUMBER

Final report on one phase of the NRL problem.

(6) 4. TITLE (and Subtitle): OCEAN ENVIRONMENTAL INFLUENCES OF TEMPERATURE AND MECHANICAL STRESS ON BARE FIBER-OPTIC SENSORS OF ACOUSTIC PRESSURES, PART I.

5. TYPE OF REPORT & PERIOD COVERED

6. PERFORMING ORG. REPORT NUMBER

(10) 7. AUTHOR(s): Sam Hanish

(11) 6 Jan 81

8. CONTRACT OR GRANT NUMBER(s): (12) 66

9. PERFORMING ORGANIZATION NAME AND ADDRESS

Naval Research Laboratory
Washington, DC 20375

10. PROGRAM ELEMENT, PROJECT, TASK AREA & WORK UNIT NUMBERS

Program Element 62711N
Project ZF11-121-004
NRL Problem 81-F100-0-0

11. CONTROLLING OFFICE NAME AND ADDRESS

Defense Advanced Research Projects Agency
1400 Wilson Boulevard
Arlington, VA 22209

12. REPORT DATE

January 6, 1981

13. NUMBER OF PAGES

65

14. MONITORING AGENCY NAME & ADDRESS (if different from Controlling Office)

(16) F11121

15. SECURITY CLASS. (of this report)

UNCLASSIFIED

15a. DECLASSIFICATION/DOWNGRADING SCHEDULE

16. DISTRIBUTION STATEMENT (of this Report)

(17) ZF11121004

Approved for public release; distribution unlimited.

17. DISTRIBUTION STATEMENT (of the abstract entered in Block 20, if different from Report)

18. SUPPLEMENTARY NOTES

19. KEY WORDS (Continue on reverse side if necessary and identify by block number)

Fiber-optic sensor
Fiber-optic hydrophone
Temperature and stress dependence of fiber-optic hydrophones

20. ABSTRACT (Continue on reverse side if necessary and identify by block number)

A theoretical analysis is made of the signal-to-noise ratio of a fiber-optic hydrophone based on general forms of power spectra of random environmental noise. The signal is a single-frequency acoustic pressure wave. The noise is a sum of shot noise, laser jitter, environmental temperature fluctuations and environmental mechanical-stress fluctuations. Environmental effects are discussed in terms of autocorrelation functions and power spectra. Explicit formulas are derived for the case of Gaussian autocorrelations.

(Continued)

DD FORM 1 JAN 73 1473 EDITION OF 1 NOV 65 IS OBSOLETE
S/N 0102-014-6601

SECURITY CLASSIFICATION OF THIS PAGE (When Data Entered)

251750

4F

20. ABSTRACT (Continued)

A detailed investigation is undertaken of the effects of temperature fluctuations in the ocean on the phase stability of the signal beam. Both large-scale temperature fluctuations caused by internal waves and small-scale fluctuations caused by velocity turbulence and thermal diffusion are considered. Numerical calculations are made of specific cases of interest. It is concluded that the stability of phase is either strongly affected or moderately affected, depending on the length of the fiber exposed to the medium, the depth in the ocean, the track length of towed sensors, the time of exposure in moored sensors, and the characteristics of built-in instrumental spectral windows.

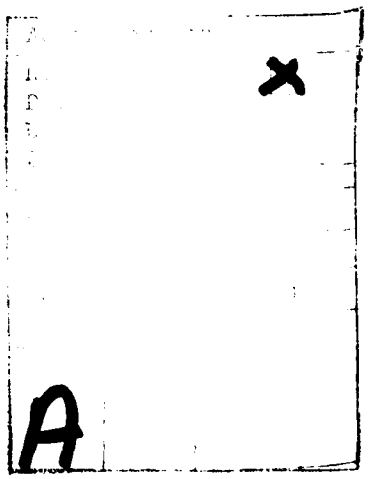

CONTENTS

SUMMARY

Laser light conducted by optical fibers in a liquid medium is modulated by acoustic pressures. This phenomenon is exploited to make an acoustic sensor of underwater sound by demodulating the light through a heterodyning procedure. In application to underwater detection of ocean acoustic signals the problem arises as to the response of bare fibers to fluctuations of ocean temperature. Quantitative estimates are necessary of the extreme case where the fibers are bare, the temperature is instantaneously sensed throughout the fiber, and statistical equilibrium is present. The effects of conductivity are deliberately omitted.

The procedure for making these estimates followed these steps: First, a derivation was made of a formula for the signal/noise ratio of a generic fiber-optic hydrophone which included all noise contributions, shot noise, amplifier noise, Johnson noise, laser jitter noise, environmental temperature noise, and environmental mechanical stress noise; this report calculates numerical estimates of the last two types of noise to show their phase-distorting effects. Second, the bare fiber-optic sensor, in the form of a single length of fiber, was reviewed in terms of its instrument temporal and spatial windowing. Numerical estimates are shown to be strongly dependent on how much of the wavenumber—frequency power spectrum of internal waves is accepted by these windows. Third, the temperature fields of the ocean were categorized by adoption of pertinent Garrett and Munk spectra of internal waves, including the effects of tow speed. It is shown from these spectra that for ordinary tow speeds the ocean temperature field is very nearly frozen, except for the very shortest and very longest wavelengths. Fourth, for specific lengths of bare fibers at specific depths quantitative estimates were made of the fiber response to ocean temperature fluctuations. The results are shown in tabular form. Briefly, the rms phase fluctuation for fibers at 100-m depth is estimated to be 4.04 rad for a 1000-m towed fiber, 3.83 rad for a 100-m dropped (i.e., vertical) fiber, and 1.6 to 19.6 rad for a moored fiber, depending on the duration of observation of internal waves. Fifth, a review was made of microtemperature scales in the ocean and quantitative estimates of their effects on phase distortion. It is shown that a fiber 0.4 cm long at a depth of 30 to 60 m exhibits a phase distortion of 1.7 rad, while a 0.01-cm fiber exhibits a 0.29-rad distortion, all attributed to microtemperature fluctuations on bare fibers.

OCEAN ENVIRONMENTAL INFLUENCES OF TEMPERATURE AND MECHANICAL STRESS ON BARE FIBER-OPTIC SENSORS OF ACOUSTIC PRESSURES
PART I

INTRODUCTION

A fiber-optic hydrophone based on heterodyne detection consists of three essential parts: a laser, two fibers, and a photodetector. At the output of the laser the beam is split in two, and each beam is coupled to a fiber: one fiber carries the *reference beam*; the second fiber is exposed to the acoustic wavefield, which modulates the laser light to form the *signal beam*. The two fibers feed simultaneously into the photodetector, which develops an electric current component proportional to the phase difference between the two beams. This signal current is then amplified by a preamplifier, which delivers a voltage proportional to the acoustic signal.

One problem in the analysis of a fiber-optic hydrophone is to determine its *signal-to-noise* (S/N) ratio, which is a measure of its acoustic performance. A second problem is to obtain quantitative estimates of the noise induced in the signal beam by *environmental disturbances* such as temperature fluctuations and mechanical stresses. Both of these problems are investigated in this report.

PROCEDURE OF ANALYSIS

An optical fiber of length L carrying the signal beam is assumed to be disturbed by environmental factors. It is desired to calculate the effect of these disturbances on the stability of the phase of the signal beam and from this to determine the S/N ratio of the fiber. The procedure of analysis used in this report to make these calculations will be based on autocorrelation functions and power spectra of the random environmental disturbances. To illustrate this procedure, let the disturbance be a random temperature field $\delta\theta(x, t)$. The corresponding random phase $\Delta\phi(x, t)$ of the signal caused by this field is derived from it in the following way.

Relation Between Mean-Square Phase Fluctuation and Mean-Square Temperature Fluctuation

Let $\delta\phi^{(j)}$ be the j th realization of the phase fluctuation over a length L of a fiber due to temperature fluctuation $\delta\theta^{(j)}(x)$ at a point x of the fiber. Then

$$\delta\phi_L^{(j)} = \int_0^L C_\theta(x)\, \delta\theta^{(j)}(x)\, dx,$$

where C_θ is a temperature-to-phase conversion factor, with units (rad/°C)/m. Assume $C_\theta(x) = C_\theta =$ const and define a quantity X such that

$$\delta\phi_L^{(j)} = C_\theta X^{(j)}, \quad X^{(j)} = \int_0^L \delta\theta^{(j)}(x)\, dx.$$

Now the mean-squared value of $\delta\phi_L$ is

$$<\delta\phi_L^2> = C_\theta^2 \int_0^L \int_0^{x'} <\delta\theta(x)\, \delta\theta(x')> dx dx'.$$

But by the definition of autocorrelation

$$<\delta\theta(x)\delta\theta(x')> = <\delta\theta^2>\, \rho_{\delta\theta}(x - x'),$$

Manuscript submitted on April 29, 1980.

in which $<\delta\theta^2>$ is the variance and $\rho_{\delta\theta}(x - x')$ is the nondimensional autocorrelation of the random function $\delta\theta(x)$. Now following Taylor [1] one can write

$$\int_0^{x'} <\delta\theta(x)\,\delta\theta(x')> dx = <\delta\theta(x')\,X> = \frac{1}{2}\frac{d}{dx'}<X^2>.$$

Since we shall always take ρ to be an even function, we write $\rho(x - x')dx = \rho(\xi)d\xi$. Then

$$<X^2> = 2<\delta\theta^2>\int_0^L \int_0^{x'} \rho(\xi)d\xi\,dx'.$$

Two limiting forms are immediately available:

- If L is short enough for $\rho(\xi)$ to be about unity, then

$$<X^2> = 2<\delta\theta_L^2>\int_0^L \int_0^{x'} d\xi\,dx' = <\delta\theta_L^2>L^2.$$

This is the *coherent* case.

- If L is so long that many uncorrelated inhomogeneities of temperature are present over the fiber, then there is an *integral scale* L_c such that

$$<X^2> = 2<\delta\theta_L^2>\int_0^\infty \rho(\xi)d\xi\int_0^L dx' = 2<\delta\theta_L^2>L_cL.$$

This is the *incoherent* case. Between these extremes we can write another form, obtainable from the above forms by interchange of order of integration [2]:

$$<X^2> = 2\,<\delta\theta_L^2>\,L\int_0^L \left(1 - \frac{\xi}{L}\right)\rho_{\delta\theta}(\xi)\,d\xi.$$

In the following applications we shall be mainly interested in cases where $L >> L_c$. The mean-square phase fluctuation due to temperature fluctuation per unit of length L then becomes

$$\frac{\sqrt{<\delta\phi_L^2>}}{L} = C_{\theta L}\sqrt{2\frac{L_c}{L}}\sqrt{<\delta\theta_L^2>},\quad L_c << L.$$

In the literature of temperature statistics in the ocean, the integral scale L_c of temperature fluctuations is only sparsely known. Since the formula for $<\delta\phi_L^2>$ is valid for $L_c << L$, we shall have to resort to several approaches to overcome the limited information about L_c:

- Wherever it is known, we use L_c.

- When L_c is not known, we can assume a special case,

$$2LL_c = O(1)\mathrm{m}^2,\quad L_c << L,$$
$$\sqrt{<\delta\phi_L^2>} = C_{\theta L}\sqrt{<\delta\theta_L^2>}.$$

- When L_c is not known, we assume that the autocorrelation is Gaussian, $\rho(\xi) = e^{-\xi^2/2L_{\delta\theta}}$;

then

$$<\delta\phi_L^2> = C_{\theta L}^2\,<\delta\theta^2>\,[2LL_{\delta\theta} - 2\,L_{\delta\theta}^2\,(1 - e^{-L^2/2L_{\delta\theta}^2})]^{1/2}.$$

The correlation length $L_{\delta\theta}$ must be assumed. (See Appendix A.)

We prefer the second approach and shall use it in calculations below. A similar derivation may be made for the case of rms phase fluctuation due to time-varying temperature fluctuations for nearly incoherent summation,

$$\frac{\sqrt{<\delta\phi_T^2>}}{T} = C_{\theta T}\sqrt{\frac{2T_c}{T}}\sqrt{<\delta\theta_T^2>},$$

where

$C_{\theta T}$	=	conversion constant	(units: $°C^{-1}\cdot s^{-1}$),
T_c	=	correlation time of $\delta\theta(t)$	(units: s),
T	=	integration time	(units: s), and
$<\delta\theta_T^2>$	=	variance of $\delta\theta(t)$	(units: $°C^2$).

When both temporal and spatial effects are considered together, the combined variance $<\delta\theta_{LT}^2>$ must be used. The result is

$$\frac{\sqrt{\delta\phi_{LT}^2>}}{LT} = C_{\theta LT}\sqrt{2\frac{L_c}{L}\frac{T_c}{T}}\sqrt{<\delta\theta_{LT}^2>},$$

where $C_{\theta LT}$ = conversion constant, in (rad/°C)/(m/s). This formula applies only when $L_c << L$ and $T_c << T$. Again, when T_c is not known we may choose

$$2TT_c = O(1)s^2, \quad T_c << T,$$

so that

$$\sqrt{<\delta\phi_T^2>} = C_{\theta T}\sqrt{<\delta\theta_B^2>}.$$

A more drastic assumption is

$$2LL_c\,TT_c = O(1)\ m^2\cdot s^2,$$

so that

$$\sqrt{<\delta\phi_{LT}^2>} = C_{\theta LT}\sqrt{<\delta\theta_{LT}^2>}.$$

It is to be noted that rms phase fluctuations can be reported per unit length, per unit time, or per unit length per unit time only if the correlation length and correlation time are known. If the assumptions are made that $2LL_c = O(1)m^2$ and $2TT_c = O(1)s^2$, then the rms phase fluctuation refers to the entire length or entire duration of the measurements procedure.

Discussion: The variance $<\delta\theta^2>$ in electrical terms is the averaged ac power over a specified sample size of finite dimension:

$$\int_0^L <|\delta\theta|^2>\,dx = L\ <\delta\theta_L^2>.$$

It is related to the power spectrum $\delta S_{\delta\theta}(\alpha)$ of the random process $\delta\theta(x)$ in that $\delta S_{\delta\theta}(\alpha)$ shows how the variance is distributed over wavenumber. In numerical calculations the value to be assigned to the space-averaged variance will be determined in this report by integration of the power spectrum over a band of wavenumbers. Because L is finite, the power contained in spatial frequencies whose wavelengths are much larger than L will not be present in $<\delta\theta_L^2>$. Hence the allowable band of wavenumbers must be finite. Furthermore there is an *additional limit* on the thermal energy in the fiber over the length L. It is found in $<X^2>$:

$$<X^2> = <\int_0^L\int_0^x \delta\theta(x)\,\delta\theta(x')\,dxdx'>$$
$$= 2\ <\delta\theta^2>\int_0^L\int_0^{x'}\rho(\xi)\ d\xi\,dx'.$$

This shows that lack of correlation between the temperature at the beginning and at the end of the fiber reduces the thermal energy in the fiber.

In summary, the method used in this report is to calculate $<\delta\theta^2>$ over a finite band of spatial wavenumbers (or temporal frequencies) and then to evaluate the effect of correlation.

We relate these results to those of Garrett and Munk GM72 [3]; the appropriate formula is that of their footnote on page 237,

$$<\delta\theta^2(\Delta\alpha)> = \int_{\Delta\alpha} \hat{F}_T(\alpha)\, d\hat{\alpha} = \int_{\Delta\alpha} \left(\frac{d\theta}{dy}\right)^2 \hat{F}_\zeta(\alpha)\, d\hat{\alpha},$$

in which the units of $\hat{F}_\zeta(\alpha)$ are $(m^2/cycle)/m$. Thus the mean-squared phase is

$$<\delta\phi^2(\Delta\alpha)> = C_\theta^2\ 2LL_C \int \left(\frac{d\theta}{dy}\right)^2 \hat{F}_\zeta(\alpha)\, d\hat{\alpha}\ \text{(units: rad}^2\text{)}.$$

Letting, as before, $2LL_c = O(1)m^2$, we choose a fiber of length L, index of refraction n, and laser wavelength $\lambda_0 = 2\pi/k_0$, for which C_θ is known (see later sections), and write

$$<\delta\phi^2(\Delta\alpha)> = k_0 n\left(\frac{1}{n}\frac{\partial n}{\partial\theta} + \frac{1}{L}\frac{\partial L}{\partial\theta}\right)\sqrt{<\delta\theta^2(\Delta\alpha)>}.$$

In these formulas the integration limits enclose a band of wavenumbers $\Delta\alpha$ wide. The limits can be extended to plus or minus infinity if a window $W(x)$ is used to represent the effects of measurement restrictions or signal-processing restrictions. A formal discussion of windows is found in Appendix B. For the purposes of this report we choose a simpler approach. Let $W(x)$ (units: m^{-1}) be a spatial window modeled as an impulse response of a filter. Then the Fourier transform of this filter is

$$W(\alpha) = \frac{1}{2\pi}\int_{-\infty}^{\infty} W(x)\, e^{-i\alpha x}\, dx \quad \text{(units: none)}.$$

Thus the band-limited variance of $\delta\phi$ is

$$<\delta\phi_L^2> = 2LL_c\ C_{\theta L}^2 \int_{-\infty}^{\infty} \left(\frac{d\theta}{dy}\right)^2 \hat{F}_\zeta(\alpha)|W(\alpha)|^2\, d\alpha \quad \text{(units: rad}^2\text{)}.$$

In a similar way, if $w(t)$ is a temporal window, then

$$W(\omega) = \frac{1}{2\pi}\int_{-\infty}^{\infty} w(t)e^{-i\omega t}dt$$

and

$$<\delta\phi_T^2> = 2\ C_{\theta T}^2\ TT_c \int_{-\infty}^{\infty} \left(\frac{d\theta}{dy}\right)^2 \hat{F}_\zeta(\omega)\ |W(\omega)|^2\, d\omega,$$

where $\hat{F}_\zeta(\omega)$ is the temporal power spectrum of internal waves and $|W(\omega)|^2$ is the filter transfer function.

The procedure of analysis summarized above depends very strongly on the existence of measured power spectra of internal waves in the ocean. The precision of these measurements and their ultimate significance under the conditions of local space and time make them only approximate. In most cases good approximations are available. These will be used in later sections of this report to made numerical estimates of environmental noise, which will ultimately be used to determine a signal-to-noise figure of merit S/N of the fiber-optic sensor.

The mathematical form of S/N points the way toward the appropriate form to be given to the environmental noise effect. We now turn to an investigation of the required general expression for S/N of a fiber-optic hydrophone.

SIGNAL/NOISE RATIO OF FIBER-OPTIC HYDROPHONES

Photodetector Current

In a laser heterodyne detection system the superposition on the surface of the photodetector of the reference beam, with intensity I_r, and the signal beam, with intensity I_s, can be modeled on the

theory of partially coherent light [4]. In this theory the total intensity of two superimposed beams which differ in phase by $\Delta\phi$ is

$$I_{rs} = I_r + I_s + 2|\gamma_{rs}|\sqrt{I_r I_s}\cos[\alpha_{rs}(\tau) - \Delta\phi] \quad \text{(units: V·A/m}^2\text{)},$$

in which γ_{rs} is the complex degree of mutual coherence, $|\gamma_{rs}|$ is its modulus, and

$$\alpha_{rs}(\tau) = \arg\gamma_{rs} + 2\pi\bar{f}\tau,$$

where $\bar{f}$ is the mean frequency of the laser and τ is spatial path difference. In terms of the laser-beam wavenumber k, one can write the phase difference as a path difference Δx,

$$\Delta\phi = k\,\Delta x \qquad \text{(units: rad)}.$$

If the laser field is represented by the analytic signal $V(t)$, then by definition

$$\gamma_{rs}(\tau) = \frac{\Gamma_{rs}(\tau)}{\sqrt{\Gamma_{rr}(0)}\sqrt{\Gamma_{ss}(0)}} = \frac{\Gamma_{rs}(\tau)}{\sqrt{I_r}\sqrt{I_s}}$$

and

$$\Gamma_{rs}(\tau) = \langle V_r(t+\tau)\, V_s^*(t)\rangle \qquad \text{(units: V·A/m}^2\text{)},$$

in which $\langle\ \rangle$ signifies statistical average in time, Γ_{rr} is the autocorrelation of the random variable $V(t)$, Γ_{rs} is the crosscorrelation of the random variables V_r and V_s, and τ is the delay time. Since $|\gamma_{rs}|\cos[\alpha_{rs}(\tau) + \Delta\phi]$ is a real number, $\mathrm{Re}\,\gamma_{rs}$, it is a measurable quantity, namely,

$$\mathrm{Re}\,\gamma_{rs} = \frac{I_{rs} - I_r - I_s}{2\sqrt{I_r}\sqrt{I_s}}.$$

The total intensity I_{rs} thus is a sum of coherent and incoherent parts. It is justifiable to assume that over sufficiently long time the random part is uniformly incident over the area of illumination of the photodetector. By integration over this area the total light power incident on the collecting surface becomes

$$P_{rs} = P_r + P_s + 2|\gamma_{rs}|\sqrt{P_r P_s}\cos[\alpha_{rs}(t) - \Delta\phi] \quad \text{(units: V·A)}.$$

This light power generates a photodetector current of time-average value

$$\langle i\rangle = D\langle P_{rs}\rangle \qquad \text{(units: A)},$$

in which D is the photodetector conversion factor (units: V^{-1} or A/V·A). To emphasize partial coherency, it is useful to write this current in the form

$$\langle i\rangle = |\gamma_{rs}|\, D[P_r + P_s + 2\sqrt{P_r P_s}\cos(\alpha_{rs} - \Delta\phi)] + (1 - |\gamma_{rs}|)\, D(P_r + P_s).$$

The first term represents the coherent superposition of two beams of powers $|\gamma_{rs}|P_r$ and $|\gamma_{rs}|P_s$, while the second term represents incoherent superposition of two beams of powers $(1 - |\gamma_{rs}|)P_r$ and $(1 - |\gamma_{rs}|)P_s$. This distinction between coherent and incoherent parts of the photodetector current will be used to advantage in further developments.

The phase $\Delta\phi$ is the sum of two terms: a nonacoustic phase $\Delta\phi_0$ and an acoustically induced phase $\Delta\phi_A$. In the absence of the latter the average photodetector current can be written just as shown above with $\Delta\phi$ replaced by $\Delta\phi_0$. It is then essentially a sum of dc terms, I_{ph} (units: A). In the presence of an acoustic signal which varies sinusoidally in time, the cosine term becomes

$$\cos(\alpha_{rs} - \Delta\phi_0 - \Delta\phi_A) = \cos(\alpha_{rs} - \Delta\phi_0)\cos\Delta\phi_A + \sin(\alpha_{rs} - \Delta\phi_0)\sin\Delta\phi_A.$$

If we assume that $\sin\Delta\phi_A \approx \Delta\phi_A$, then there exists a time-varying photodetector component current,

$$\langle i_{AC}\rangle \approx 2D|\gamma_{rs}|\sqrt{P_r P_s}\sin[\alpha_{rs}(\tau) - \Delta\phi_0]\,\Delta\phi_A(t).$$

The nonacoustic phase $\Delta\phi_0$ may contain a random component of time $\Delta\phi_0(t)$ caused by environmental disturbances. In this case, when there is no useful acoustic signal,

$$\cos[\alpha_{rs} - \Delta\phi_0 - \Delta\phi_0(t)] = \cos(\alpha_{rs} - \Delta\phi_0)\cos\Delta\phi_0(t) + \sin(\alpha_{rs} - \Delta\phi_0)\sin\Delta\phi_0(t).$$

When the *fixed* phase $\alpha_{rs} - \Delta\phi_0$ is adjusted to be $\pi/2$, as is customary, there remains a random component of photodetector current

$$i_{\Delta\phi_0} \approx 2D\ |\gamma_{rs}|\ \sqrt{P_r P_s}\ \sin[\Delta\phi_0(t)].$$

The probability distribution of $i_{\Delta\phi_0}$ is determined by the sine of the probability distribution of $\Delta\phi_0(t)$. In later sections of this report we shall consider $\Delta\phi_0(t)$ to be caused by random temperature fluctuations, and we shall derive numerical estimates of its magnitude in typical ocean environments.

Coherent and Incoherent dc Photodetector Currents

The time-averaged dc photodetector currents contribute noise in the detection circuits. As noted above these currents are the sum of coherent and incoherent terms. The incoherent terms consist of three contributions:

- scattering of laser light in the fiber by Bragg reflection from thermally induced acoustic plane-wave trains (Brillouin scattering);
- scattering from mass-density fluctuations caused by random motion of the molecules of glass in the fiber whenever the wavelength of the incident laser beam is much smaller than the size of the molecules (Rayleigh scattering); and
- scattering from spherical (or irregular) inhomogenities where the characteristic dimension is larger than, or comparable with, a wavelength of the incident light (Mie scattering).

Thus, the incoherent part of the dc current may be explicitly written in the form

$$\begin{aligned}(I_{ph})_{\text{incoh}} &= D(1 - |\gamma_{rs}|)(P_r + P_s) \\ &= D\,(P_{rB} + P_{rR} + P_{rM} + P_{sB} + P_{sR} + P_{sM}) \qquad \text{(units: A)},\end{aligned}$$

where the subscripts B, R, and M refer to Brillouin, Rayleigh, and Mie scattering, respectively. The coherent part of the dc current has already been formalized above:

$$(I_{ph})_{\text{coh}} = |\gamma_{rs}|D[P_r + P_s + 2\sqrt{P_r P_s}\cos(\alpha_{rs} + \Delta\phi_0)] \qquad \text{(units: A)}.$$

Here all terms are non-time-varying ones.

Noise in the Photodetector and Associated Preamplifier Circuitry

Shot Noise

Shot noise power is determined from the dc current I_{ph} of the photodetector explicitly formulated above and two other currents: a dc current due to background light (I_{BK}) and the dc dark current which enters the detector circuit (I_D). If the photodetector has an internal current gain G the total shot noise will be given by

$$2e[(I_{ph})_{\text{coh}} + (I_{ph})_{\text{incoh}} + I_{BK} + I_D] < G^2 > \qquad \left[\text{units: } \frac{\text{A}^2}{\text{Hz}}\right],$$

in which e is the electronic charge and $< G^2 > = < G >^2 F(G)$, where $F(G)$ accounts for an additional multiplication (or gain) due to the nonlinear properties of gain development inside the photodetector. The value of $F(G)$ is 0.5 to 3.0, depending on the type of detector used [5].

Thermal Noise

The load resistor R_L of the detector generates Johnson noise W_J when a thermally induced current i_T flows through it:

$$W_J = \langle i_T^2 \rangle \, R_L .$$

This noise power in a band δf units wide at absolute temperature Θ is

$$W_J = 4k\Theta \, \delta f \qquad \text{(units: V·A)},$$

where $k = 1.38 \times 10^{-23}$ J/K (Boltzmann's constant). The noise density is thus

$$\frac{\langle i_T^2 \rangle}{\delta f} = \frac{4k\Theta}{R_L} \qquad \left[\text{units: } \frac{\text{A}^2}{\text{Hz}}\right].$$

This noise component is additive to the shot noise formulated above.

Laser Jitter Noise

Laser beams have associated with their steady intensity I a corresponding fluctuating intensity δI. This is the laser jitter. It generates in the photodetector a noise current $i_J(t)$. If a data record T seconds long of this current is Fourier analyzed it will have a power spectral density $|I_J(\omega)|^2$ and a power spectral density *factor*, defined here to be the quantity

$$\frac{2\pi}{T} |I_J(\omega)|^2 ,$$

in which $I_J(\omega)$ (units: A·s) is the Fourier transform of $i_T(t)$ over the duration of the finite sampling time. The choice of Fourier transform is explained in Appendix C. The mean-squared value of $i_J(t)$ is then obtained by integration over the band of frequencies spanned by $I_J(\omega)$ in the power spectral density factor:

$$\langle i_J^2(\Delta\omega) \rangle = \int_{\Delta\omega} \frac{2\pi}{T} \, |I_J(\omega)|^2 \, d\omega \qquad \text{(units: A}^2\text{)}.$$

A convenient way of deriving the power spectral density factor is through use of the autocorrelation $\Upsilon_J(\tau)$ of $i_J(t)$:

$$\frac{2\pi}{T} |I_J(\omega)|^2 = \frac{1}{2\pi} \int_{-\infty}^{\infty} e^{i\omega\tau} \, \Upsilon(\tau) \, d\tau ,$$

where

$$\Upsilon(\tau) = \frac{1}{T} \int_T i_J(t) \, i_J(t + \tau) \, dt \qquad \text{(units: A}^2\text{)}.$$

Typical forms of $\Upsilon_J(\tau)$ are discussed in a later section of this report.

Environmental Noise

Assume that the environment generates a random thermal disturbance and a random mechanical disturbance of the fiber. Let one of these disturbances be $\delta\epsilon(\mathbf{r},t)$, meaning it is a spatial and temporal fluctuation of an environmental parameter (temperature or mechanical stress). The power spectral density factor of this random function over finite volume V and finite time T is then defined to be

$$(2\pi)^4 \, \frac{|E(\mathbf{K}, \omega)|^2}{VT},$$

in which the quantity

$$E(\mathbf{K}, \omega) = \int\int_{-\infty}^{\infty} \delta\epsilon(\mathbf{r}, t) e^{i\omega t - i\mathbf{K}\cdot\mathbf{r}} \, \frac{dt}{2\pi} \, \frac{d\mathbf{r}}{(2\pi)^3}$$

is the Fourier transform of $\delta\epsilon(\mathbf{r}, t)$ (Appendix C). The mean-square value of $\delta\epsilon$ over these intervals is

$$<\delta\epsilon^2> = \iint_{VT} (2\pi)^4 \frac{|E(\mathbf{K}, \omega)|^2}{VT} d^3\mathbf{K}\, d\omega.$$

A convenient way of deriving the power spectral density of $\delta\epsilon$ is through use of the autocorrelation $\Upsilon_{\delta\epsilon}(\mathbf{d}, \tau)$:

$$\frac{1}{(2\pi)^4} \iint_{VT} \Upsilon_{\delta\epsilon}(\mathbf{d}, \tau)\, e^{i\omega t - i\mathbf{K}\cdot\mathbf{d}}\, d\tau\, d\mathbf{d} = (2\pi)^4 \frac{|E(\mathbf{K}, \omega)|^2}{VT},$$

where

$$\Upsilon_{\delta\epsilon}(\mathbf{d}, \tau) \to \frac{1}{VT} \int_{-\infty}^{\infty}\int \delta\epsilon(\mathbf{r}, t)\delta\epsilon(\mathbf{r} + \mathbf{d}, t + \tau)\, dt\, d^3\mathbf{d}.$$

The power spectral density per unit of bandwidth can be derived from these formulas by integration over wavenumber:

$$\frac{2\pi}{T}|E(\omega)|^2 = \int_{\mathbf{K}} (2\pi)^3 \frac{|E(\mathbf{K}, \omega)|^2}{V} d^3\mathbf{K}.$$

By a linear conversion factor the units of this parameter can be made $A^2{\cdot}s$. In most applications the spatial part of the spectrum is considered essentially one-dimensional. Then the power spectral density factor of $\delta\epsilon(x\, t)$ becomes

$$\frac{(2\pi)^2 |E(\alpha, \omega)|^2}{LT},$$

where

$$E(\alpha, \omega) = \iint \delta\epsilon(x, t)\, e^{i\omega t - i\alpha x} \frac{dt}{2\pi} \frac{dx}{2\pi}.$$

The mean-square value of $\delta\epsilon(x, t)$ is obtained from this by integration:

$$<\delta\epsilon^2> = \iint_{LT} (2\pi)^2 \frac{|E(\alpha, \omega)|^2}{LT} d\alpha\, d\omega.$$

Also one can form the power spectral density factor per unit of frequency bandwidth,

$$\frac{2\pi}{T}|E(\omega)|^2 = \int_{\Delta\alpha} (2\pi) \frac{|E(\alpha, \omega)|^2}{L} d\alpha.$$

Again by a linear conversion factor the units of this parameter can be made $A^2{\cdot}s$.

In all cases the quantity $\sqrt{<\delta\epsilon^2>}$ is the desired representation of the environmental disturbance, averaged over space and time. The root-mean-square amplitude of fluctuation in the phase of the laser signal beam is then desired to be

$$\Delta\phi_{\text{rms}} = A_\epsilon \sqrt{<\delta\epsilon^2>}, \quad A_\epsilon = \text{const.}$$

However, since the goal of this analysis is to estimate the noise current in the photodetector caused by environmental disturbances, the quantity actually calculated is

$$<i_\epsilon^2> = B_\epsilon\, <\delta\epsilon^2>, \quad B_\epsilon = \text{const},$$

in units of A^2. For purposes of relating environmental noise to other noises described above, it is convenient to represent it in the form of noise per unit bandwidth:

$$\frac{<i_\epsilon^2>}{\delta\omega} = C_\epsilon\, <\delta\epsilon^2(\omega)>, \quad C_\epsilon = \text{const.}$$

Examples of the application of these formulas to environmental disturbances which affect the transmission of light in fibers are given below. We consider here the effect of these disturbances on the phase of the laser light.

Let L be the length of a fiber which is acting as a transmission path for a laser beam. As the light travels from the origin to L its phase is altered by an amount

$$\phi = \int_0^L k_0(x)\, n(x)\, dx \quad \text{(units: rad)},$$

where

$$k_0(x) = \text{background wavenumber} = 2\pi/\lambda_0(x) \quad \text{(units: } \mathrm{m}^{-1}\text{)}$$

and

$$n(x) = \text{index of refraction} \quad \text{(units: none)}.$$

A simple case occurs when $k_0 n$ is a constant along the transmission path. Then

$$\phi = k_0 n L.$$

Now assume that the fiber is acted upon by a random environmental disturbance, say mechanical stress, which is represented, for convenience in this report, as a scalar pressure δS_p (units: $\mathrm{N \cdot m^{-2}}$) normal to the surface of the fiber, or as a scalar torsion δS_τ. The change in phase to first order in the change in stress is

$$\delta\phi^* = \left(\frac{\partial k_0}{\partial \delta S}\, n + k_0 \frac{\partial n}{\partial \delta S} + k_0 n_L \frac{\partial L}{\partial \delta S} \right) \delta S \quad \text{(units: } \mathrm{m}^{-1}\text{)},$$

in which the asterisk indicates "per unit length." For scalar pressure changes the last term in the parentheses can be written in terms of the bulk compressibility,

$$K^{-1} \equiv -\frac{1}{\delta S_p} \left(\frac{\Delta V}{V} \right) \quad \text{(units: } \mathrm{m^2 \cdot N^{-1}}\text{)}.$$

If ΔL represents the change in one dimension, then for a three-dimensional isotropic body

$$K^{-1} = -\frac{1}{\delta S_p} \frac{\Delta L}{L} \times 3.$$

Replacing $\partial L/\partial S_p$ by $\Delta L/\delta S_p$, and assuming $\partial k_0/\partial \delta S_p \approx 0$, one finds

$$C_s \equiv \frac{\delta\phi^*}{\delta S_p} = \left(\frac{1}{n} \frac{\partial n}{\partial S_p} - \frac{K^{-1}}{3} \right) k_0 n \quad \left[\text{units: } \frac{\text{rad} \cdot \text{m}^2}{\text{N} \cdot \text{m}} \right].$$

Following the procedure explained earlier in the section "Procedure of Analysis" the average value of the fluctuation in $\delta\phi$ is

$$\delta\phi_{L\,\mathrm{rms}} = \sqrt{\langle \delta\phi_L^2 \rangle} = C_s \sqrt{\langle \delta S_p^2 \rangle\, 2LL_c}$$

$$= \left(\frac{1}{n} \frac{\partial n}{\partial S_p} - \frac{K^{-1}}{3} \right) k_0 n \sqrt{\langle \delta S_p^2 \rangle} \quad \text{(units: rad)},$$

assuming that $2LL_c = O(1)\ \mathrm{m}^2$. A similar formula can be constructed for changes in scalar torsional stresses. We assume that a constant twisting moment M induces a constant angle of twist ϕ in a fiber of circular cross section with polar moment of inertia I_0,

$$M = GI_0 \frac{\phi}{L} \quad \text{(units: N·m)},$$

in which G is the modulus of rigidity (units: $\mathrm{N \cdot m^{-2}}$), and the units of I_0 are m^4. A change in M induces a change in ϕ:

$$\Delta M = GI_0 \frac{\Delta\phi}{L}.$$

We assume a linear relation exists between a change in fiber length and a change in angle of twist. By definition,

$$\alpha = \frac{\Delta L}{\Delta\phi} \quad \text{(units: m)}.$$

Hence,

$$\frac{\Delta L}{L\Delta M} = \frac{\alpha}{GI_0}.$$

Thus, for random twisting moments δM,

$$\delta\phi_{L\,\mathrm{rms}} = \sqrt{<\delta\phi_L^2>} = \left(\frac{1}{n}\frac{\partial n}{\partial M} + \frac{\alpha}{GI_0}\right) k_0 n \sqrt{<\delta M^2>\, 2LL_c}.$$

This is a one-dimensional statement. In three dimensions we repeat the above analysis to obtain the effects of random torsional stress δS_τ:

$$\sqrt{<\delta\phi^2>} = \left(\frac{1}{n}\frac{\partial n}{\partial S_\tau} - \frac{K_G^{-1}}{3}\right) k_0 n \sqrt{<\delta S_\tau^2>\, 2LL_c},$$

in which

$$K_G^{-1} \equiv -\frac{1}{V}\left(\frac{\Delta V}{\Delta S_\tau}\right).$$

In both cases the symbol δ is used to indicate fluctuations. The constant C_s is directly related to special constants in the theory of photoelasticity, values of which appear as C in Part II of this report, NRL Report 8425.

Laser Jitter and Environmentally Induced Noise for Gaussian Correlated Fields

In the section "Environmental Noise" it was found that the noise current in the photodetector current can be obtained from the mean-square environmental disturbance $<\delta\epsilon^2>$ averaged over space and time. This quantity in turn can be calculated from a knowledge of the power spectral density $|E(\mathbf{K}, \omega)|^2$ of $\epsilon(\mathbf{K}, t)$. Again, as noted earlier, a convenient way of calculating spectra is through the use of autocorrelation functions. We treat now several cases.

Power Spectral Density of Mechanical Stress and Associated Noise

Let the environmental disturbance be a random mechanical stress which is represented in reduced form as a scalar $\delta S(\mathbf{r}, t)$. The autocorrelation function over all space and time is

$$\Upsilon_s(\mathbf{l}, \tau) = \lim_{\substack{V\to\infty \\ T\to\infty}} \left[\frac{1}{VT}\int_V\int_T \delta S(\mathbf{r}, t)\delta S(\mathbf{r}+\mathbf{l}, t+\tau)\,dvdt\right].$$

In all applications to real phenomena both V and T are finite. The mean-square fluctuation, or *variance*, is the value over the whole V and the whole T:

$$<\delta S^2> = \Upsilon_s(0, 0) = \frac{1}{VT}\int_V\int_T \delta S^2(\mathbf{r}, t)\,dvdt \quad \text{(units: } \mathrm{N^2\cdot m^{-4}}).$$

Because of instrumental and experimental limitations, not all space and not all time can be measured. There is an *effective* band of wavenumbers and an *effective* band of frequencies that are resolvable under

the conditions of test. Thus the full variance $<\delta S^2>$ is not physically reportable. To deal with a finite spatial and temporal spectrum, we utilize the full autocorrelation function. Examples are now developed.

Assume that the scalar stress field is isotropic in space, so that its autocorrelation is dependent on distance l between $\mathbf{r}$ and $\mathbf{r}'$, and not on orientation of the vector separation $\mathbf{l}$. Further assume a simple Gaussian form for both space and time dependence:

$$\Upsilon_{\delta S}(\mathbf{l}, \tau) = <\delta S^2> \exp\left[-\frac{1}{2}\left(\frac{l}{l_{cm}}\right)^2 - \frac{1}{2}\left(\frac{\tau}{\tau_{cm}}\right)^2\right] \quad \text{(units: A}^2\text{)},$$

in which henceforth we shall take the units of $<\delta S^2>$ to be the noise-current equivalent, A^2. Here l_{cm} is the correlation length of the random stress field and τ_{cm} is its correlation time. As noted earlier, the power spectral density factor is given by

$$(2\pi)^4 \frac{|\delta S(\mu, \omega)|^2}{VT} = \frac{<\delta S^2>}{(2\pi)^4} \int_V \int_T d\tau\, d^3\mathbf{l}\, e^{-\frac{1}{2}\frac{\mathbf{l}\cdot\mathbf{l}}{l_{cm}^2}} e^{-\frac{1}{2}\left(\frac{\tau}{\tau_{cm}}\right)^2} e^{-\boldsymbol{\mu}\cdot\mathbf{l}} e^{i\omega\tau},$$

in which $\boldsymbol{\mu}$ is a vector wavenumber. The integration over τ yields $\sqrt{2\pi}\,\tau_{cm} \exp[-\frac{1}{2}\omega^2\tau_{cm}^2]$. The integration over $\mathbf{l}$ is found by noting that $d^3\mathbf{l} = dL_x\, dL_y\, dL_z$ and that, because of isotropy of the stress field, $d^3\mathbf{l} \rightarrow (\sqrt{2\pi}\, l_{cm})^3 dl_x$, where dl_x is nondimensional. Thus,

$$(2\pi)^4 \frac{|\delta S(\mu, \omega)|^2}{VT} = \frac{l_{cm}^3 \tau_{cm}}{(2\pi)^2} <\delta S^2> \exp\left[-\frac{1}{2}|\boldsymbol{\mu}\cdot\boldsymbol{\mu}|l_{cm}^2 - \frac{1}{2}\omega^2\tau_{cm}^2\right] \quad \text{(units: A}^2\cdot\text{m}^3\cdot\text{s)}.$$

By integration over a volume of effective wavenumber $\Delta\mu$ we obtain the noise power spectral density *factor* per unit bandwidth of frequency:

$$\frac{2\pi}{T}|\delta S(\omega)|^2 = \frac{<\delta S^2> l_{cm}^3 \tau_{cm}}{(2\pi)^2} \int_{\Delta\mu} \exp\left[-\frac{1}{2}|\boldsymbol{\mu}\cdot\boldsymbol{\mu}|l_{cm}^2\right] d^3\boldsymbol{\mu} \exp\left[-\frac{1}{2}\omega^2\tau_{cm}^2\right] \quad \text{(units: A}^2\cdot\text{s)},$$

in which

$$|\delta S(\omega)|^2 = \int \frac{(2\pi)^3 |\delta S(\boldsymbol{\mu}, \omega)|^2}{V} d^3\boldsymbol{\mu} \quad \text{(units: A}^2\cdot\text{s}^2\text{)}.$$

Finally, by integration over an effective band of frequencies $\Delta\omega$, one gets the mean-squared band-limited variance:

$$<\delta S^2(\Delta\mu, \Delta\omega)> = \frac{<\delta S^2> l_{cm}^3 \tau_{cm}}{(2\pi)^2} \int_{\Delta\omega} d\omega \int_{\Delta\mu} d^3\boldsymbol{\mu} \exp\left[-\frac{1}{2}|\boldsymbol{\mu}\cdot\boldsymbol{\mu}|l_{cm}^2 - \frac{1}{2}\omega^2\tau_{cm}^2\right]$$

$$= <\delta S^2> F_4(\Delta\mu, \Delta\omega) \quad \text{(units: A}^2\text{)}.$$

Here $F_4(\Delta\mu, \Delta\omega) < 1$ when $\Delta\mu$ and $\Delta\omega$ are finite, and $F_4(\Delta\mu, \Delta\omega) = 1$ when $\Delta\mu$ and $\Delta\omega$ are infinite. The subscript 4 denotes a four-coordinate system (3-space and time).

When the spatial dependency of δS is one-dimensional, the power spectral density factor is

$$(2\pi)^2 \frac{|\delta S_x(\alpha, \omega)|^2}{LT} = \frac{<\delta S^2>}{(2\pi)^2} \int_L \int_T e^{-\frac{1}{2}\left(\frac{l}{l_{cm}}\right)^2 - \frac{1}{2}\left(\frac{\tau}{\tau_{cm}}\right)^2} e^{-i\alpha l + i\omega\tau}\, d\tau\, dl$$

$$= \frac{<\delta S^2>}{(2\pi)} l_{cm}\tau_{cm} \exp\left[-\frac{\alpha^2 l_{cm}^2}{2} - \frac{\omega^2\tau_{cm}^2}{2}\right] \quad \text{(units: A}^2\cdot\text{m}\cdot\text{s)}.$$

Thus the power spectral density factor per unit bandwidth of frequency is

$$\frac{2\pi}{T}|\delta S(\omega)|^2 = \frac{<\delta S^2>}{2\pi} l_{cm}\tau_{cm} e^{-\frac{\omega^2\tau_{cm}^2}{2}} \int_{\Delta\alpha} e^{-\frac{\alpha^2 l_{cm}^2}{2}} d\alpha \qquad \text{(units: A}^2\cdot\text{s)},$$

where

$$|\delta S(\omega)|^2 = \int \frac{2\pi}{L} |\delta S(\alpha,\omega)|^2 d\alpha \qquad \text{(units: A}^2\cdot\text{s}^2\text{)}.$$

Finally, the mean-square band-limited variance of noise current due to random mechanical stress is

$$<\delta S^2(\Delta\alpha, \Delta\omega)> = \int_{\Delta\omega} \frac{2\pi}{T} |\delta S_s(\omega)|^2 \, d\omega$$

$$= \frac{<\delta S^2>}{2\pi} l_{cm}\tau_{cm} \int_{\Delta\omega} d\omega e^{-\frac{\omega^2\tau_{cm}^2}{2}} \int_{\Delta\alpha} e^{-\frac{\alpha^2 l_{cm}^2}{2}} d\alpha$$

$$= <\delta S^2> F_2(\Delta\alpha, \Delta\omega) \qquad \text{(units: A}^2\text{)}.$$

When the total dependency of the fold is one-dimensional in either space *or* time, then the mean-square bandwidth-limited variance is for space:

$$<\delta S^2(\Delta\alpha)>_x = \frac{<\delta S^2>_x l_{cm}}{\sqrt{2\pi}} \int_{\Delta\alpha} e^{-\frac{\alpha^2 l_c^2}{2}} d\alpha,$$

$$<\delta S^2>_x = \frac{1}{L}\int_L |\delta S^2(x)| \, dx,$$

and for time:

$$<\delta S^2(\Delta\omega)>_t = \frac{<\delta S^2>_t \tau_{cm}}{\sqrt{2\pi}} \int_{\Delta\omega} e^{-\frac{\omega^2\tau_{cm}^2}{2}} d\omega,$$

$$<\delta S^2>_t = \frac{1}{T}\int_T |\delta S^2(t)| dt.$$

The *total* bandwidth over frequency and wavenumber is $-\infty$ to $+\infty$.

To this point we have assumed that the autocorrelation of the random stress field is known. We can make the alternative assumption that the power spectral density is known. Then the band-limited variance can be directly calculated:

For 3-space and time: $<\delta S^2(\Delta\mu, \Delta\omega)> = \int\int_{\Delta\mu\Delta\omega} \frac{(2\pi)^4}{VT} |\delta S(\mu, \omega)|^2 d^3\mu \, d\omega$ (units: A^2),

$<\delta S^2(\infty, \infty)> = <\delta S^2>$ = variance over the entire spectrum.

For 1-space and time: $<\delta S^2(\Delta\alpha, \omega)> = \int\int_{\Delta\alpha\Delta\omega} \frac{(2\pi)^2}{LT} |\delta S(\alpha,\omega)|^2 \, d\alpha \, d\omega$ (units: A^2),

$<\delta S^2(\infty, \infty)> = <\delta S^2>$.

For 1-space: $<\delta S^2(\Delta\alpha)> = \int_{\Delta\alpha} \frac{2\pi}{L} |\delta S(\alpha)|^2 \, d\alpha$ (units: A^2),

$<\delta S^2(\infty)> = <\delta S^2>_\alpha$.

For time: $<\delta S^2(\Delta\omega)> = \int_T \frac{2\pi}{T} |\delta S(\omega)|^2 d\omega$ (units: A^2),

$<\delta S^2(\infty)> = <\delta S^2>_\omega$.

Band-limited Variance of Laser Jitter Noise

Assume that laser jitter is predominantly a temporal phenomenon. Then, using the equations derived above for Gaussian autocorrelation of the time record of jitter current in the photomultiplier, we estimate the band-limited variance of this record to be

$$<\delta i_J^2(\Delta\omega)> = \frac{<\delta J^2>_I \tau_{cJ}}{\sqrt{2\pi}} \int_{\Delta\omega} e^{-\frac{\omega^2 \tau_{cJ}^2}{2}} d\omega \quad \text{(units: A}^2\text{)},$$

where τ_{cJ} is the correlation time of the record and $\Delta\omega$ is the allowed bandwidth of the measurement system.

Band-limited Variance of Fluctuating Temperature Noise

Assume that the random temperature field is one-dimensional in space and possibly fluctuates in time and that both spatial and temporal autocorrelation are Gaussian. Then the band-limited variance of the temperature fluctuation is

$$<\delta\theta^2(\Delta\alpha, \Delta\omega)> = \frac{<\delta\theta^2>}{2\pi} l_{c\theta} \tau_{c\theta} \int_{\Delta\omega} d\omega\, e^{-\frac{\omega^2 \tau_{c\theta}^2}{2}} \int_{\Delta\alpha} d\alpha\, e^{-\frac{\alpha^2 l_{c\theta}^2}{2}},$$

where $l_{c\theta}$ and $\tau_{c\theta}$ are the correlation lengths of the spatial record and the temporal record respectively. By use of an appropriate conversion factor this becomes also the band-limited variance of the noise current generated by environmental noise.

The use of Gaussian autocorrelations for the random disturbing field may not be a best choice. In application to ocean environments a sin x/x autocorrelation has the possible advantage of greater fidelity to the random phenomena. A derivation of power spectral density factors in the sin x/x case is presented in Appendix D.

Noise Sources in the Preamplifier [5]

A preamplifier can be schematically represented as a noiseless generator with gain $A(\omega)$ and input admittance $Y_A = G_A + j\omega C_A$. It has two noise sources, a voltage noise source ν_A in series with the input terminals and a current noise source in parallel with the input terminals. The latter consists of a portion i_A which is uncorrelated with the noise voltage source and a second portion which is correlated with this source through an admittance $Y_c = \mathrm{Re}\, Y_c + j\,\mathrm{Im}\, Y_c$. We neglect this second portion. The spectral density of noise from the voltage source is $<\nu_A^2>/\delta f$ in units of V^2/Hz, and that of the current source is $<i_A^2>/\delta f$ in units of A^2/Hz.

Noise Voltage at the Output of the Preamplifier

The noise currents in the photodetector and preamplifier circuits are additive. Because of different methods of derivation, some of these noise densities are on a unit bandwidth δf basis (in cycles/s), while the remainder are on a unit angular radian $\delta\omega$ basis (in rad/s). It will be convenient in this report to keep them in separate groups. Thus, the noises $N_{\delta f}$ and $N_{\delta\omega}$ are:

On a δf basis: $N_{\delta f}$ = shot noise + amplifier noise + Johnson noise.

On a $\delta\omega$ basis: $N_{\delta\omega}$ = laser jitter noise + environmental temperature noise + environmental mechanical stress noise.

The total noise in units of V^2 at the output of the preamplifier is the sum of two terms:

$$N_{\delta f} = \int_{\Delta f} \left\{ 2e[(I_{ph})_{\text{coh}} + (I_{ph})_{\text{incoh}} + I_{BK} + I_D] <G>^2 F(G) + \frac{<i_A^2>}{\delta f} + \frac{<v_A^2>}{\delta f} |Y_I + Y_c|^2 + \frac{4kT}{R_L} \right\} \frac{|A(\omega)|^2}{|Y_I + Y_A|^2} df \qquad \text{(units: } V^2\text{)}$$

and

$$N_{\delta\omega} = \int_{\Delta\omega} \left[\frac{2\pi}{T} |\delta S_J(\omega)|^2 + \frac{2\pi}{T} \int \frac{2\pi}{L} |\delta S_{\delta\theta}(\alpha, \omega)|^2 d\alpha + \frac{2\pi}{T} \int \frac{(2\pi)^3 |\delta S_M(\mu, \omega)|^2}{V_0} d^3\mu \right] \times \frac{|A(\omega)|^2}{|Y_I + Y_A|^2} d\omega \qquad \text{(units: } V^2\text{)},$$

where

$|\delta S_J(\omega)|^2$ is the power spectrum of laser jitter (units: $A^2 \cdot s^2$),
$|\delta S_\theta(\alpha, \omega)|^2$ is the power spectrum of random temperature effects (units: $A^2 \cdot m^2 \cdot s^2$),
$|\delta S_M(\mu, \omega)|^2$ is the power spectrum of random mechanical effects (units: $A^2 \cdot m^6 \cdot s^2$),

and

V_0 is the volume of space (units: m^3).

If we assume Gaussian autocorrelations of the random disturbances, then

$$N_{\delta\omega} = \int_{\Delta\omega} \left\{ \frac{<\delta J^2> \tau_{cJ}}{\sqrt{2\pi}} e^{-\frac{\omega^2 \tau_{cJ}^2}{2}} + \frac{<\delta\theta^2> l_{c\theta} \tau_{c\theta}}{2\pi} e^{-\frac{\omega^2 \tau_{c\theta}^2}{2}} \int_{\Delta\alpha} e^{-\frac{\alpha^2 l_{c\theta}^2}{2}} d\alpha + \frac{<\delta S^2>}{(2\pi)^2} l_{CM}^3 \tau_{CM} \int_{\Delta\mu} d^3\mu \exp[-\frac{1}{2} |\mu \cdot \mu| l_{CM}^2 - \frac{1}{2} \omega^2 \tau_{CM}^2] \right\} \frac{|A(\omega)|^2}{|Y_I + Y_c|^2} d\omega.$$

Thus, in order to calculate $N_{\delta\omega}$ from assumed Gaussian autocorrelations, we are required to know the total variances of the random laser jitter, temperature, and mechanical stress field, as well as their temporal and spatial correlation lengths.

Signal Current and Voltage Sensitivity of the Hydrophone

In the section "Photodetector Current" it was seen that there is a time-varying component of photodetector current, which we call here the *signal*,

$$i_{\text{signal}} \approx 2D|\gamma_{rs}| \sqrt{P_r P_s} \sin [\alpha_{rs}(\tau) - \Delta\phi_0] \Delta\phi_A(t),$$

where $\Delta\phi_A(t)$ is the phase generated by the acoustic signal, considered to be of small enough magnitude such that $\sin \Delta\phi_A \approx \Delta\phi_A$. An oft-used design feature is to experimentally adjust $\alpha_{rs}(\tau) - \Delta\phi_0$ to be an odd multiple of $\pi/2$. This procedure maximizes the signal. Assume that this is done.

Now assume that $\Delta\phi_A(t) = \Delta\Phi_A \sin\omega_s t$. Then the rms ac component of photodetector current is

$$(i_{\text{signal}})_{\text{rms}} = 2D|\gamma_{rs}| \sqrt{P_r P_s} (\Delta\Phi_A)_{\text{rms}}.$$

The change in phase is linearly related to the acoustic pressure amplitude p_A. Hence (from earlier sections in this report) one has

$$(i_{\text{signal}})_{\text{rms}} = 2D|\gamma_{rs}|\sqrt{P_r P_s}\left(\frac{K^{-1}}{3} - \frac{1}{n}\frac{\partial n}{\partial p}\right)k_0 nL\,|p_A|_{\text{rms}}.$$

The result is characterized by the conversion of phase modulation into amplitude modulation. Actually the signal current is a statistical average, since the detection scheme is assumed only partially coherent. We therefore write it as an average, $<(i_{\text{signal}})_{\text{rms}}>$.

In photodetector procedures the signal current appears across the photodetector load resistor R_L, where it develops the signal voltage. Hence the receiving *voltage sensitivity* M is

$$M \equiv \frac{<(i_{\text{signal}})_{\text{rms}}> R_L}{|p|_{\text{rms}}} = 2DR_L|\gamma_{rs}|\sqrt{P_r P_s}\left(\frac{K^{-1}}{3} - \frac{1}{n}\frac{\partial n}{\partial p}\right)k_0 nL \qquad \text{(units: V}\cdot\text{m}^2\cdot\text{N}^{-1}\text{)}.$$

This is the sensitivity without a preamplifier. The effect of the preamplifier is discussed next.

Signal Intensity at the Output of the Preamplifier

In formulating the S/N ratio of the hydrophone we have elected to write both S and N in units of V^2 which appears across the load resistor. As noted earlier the photodetector itself amplifies the current by amount $<G>$. The preamplifier also amplifies the signal by amount $A(\omega)$. Hence the signal at the output of the preamplifier has an *intensity*

$$S = <(i_{\text{signal}})_{\text{rms}}>^2 <G>^2 \frac{|A(\omega)|^2}{|Y_I + Y_A|^2} \qquad \text{(units: V}^2\text{)},$$

where Y_I and Y_A are component electrical admittances of the photodetector amplifier circuit (Appendix E). It is to be noted that the signal is single frequency. If the signal has the character of banded noise it can be reported on a per bandwidth basis $<i_s^2>/\delta f$. Then the signal intensity appears in the form

$$S = \int_{\Delta f} \frac{<i_s^2>}{\delta f} <G>^2 \frac{|A(\omega)|^2}{|Y_I + Y_A|^2}\, df \qquad \text{(units: V}^2\text{)}.$$

Explicit Form of S/N Ratio of the Fiber-Optic Hydrophone at the Ouput of the Preamplifier

For the convenience of the reader we repeat here the explicit form of the S/N ratio of a fiber-optic hydrophone for the general case of a banded noise signal:

$$\frac{S}{N} = \frac{\displaystyle\int_{\Delta f} \frac{<i_s^2>}{\delta f} <G>^2 \frac{|A(\omega)|^2}{|Y_I + Y_A|^2}\, df}{\displaystyle\int_{\Delta f}\left\{2e[(I_{ph})_{\text{coh}} + (I_{ph})_{\text{incoh}} + I_{BK} + I_D] <G>^2 F(G) + \frac{<i_A^2>}{\delta f} + \frac{<v_A^2>}{\delta f}|Y_I + Y_c|^2 + \frac{4kT}{R_L}\right\}\frac{|A(\omega)|^2}{|Y_I Y_A|^2}\, df + \int_{\Delta\omega}\left\{\frac{2\pi}{T}|\delta S_J(\omega)|^2 + \frac{2\pi}{T}\int\frac{2\pi}{L}|\delta S_{\delta\theta}(\alpha,\omega)|^2\, d\alpha + \frac{2\pi}{T}\int\frac{(2\pi)^3}{V_0}|\delta S_M(\mu,\omega)|^2\, d^3\mu\right\}\frac{|A(\omega)|^2}{|Y_I + Y_A|^2}\, d\omega.}$$

All symbols have been defined in previous sections of this report.

INSTRUMENT WINDOWS AND THE NYQUIST LIMIT

The random environmental disturbances which affect the transmission of light through a fiber have autocorrelation functions which die away naturally with increasing spatial and temporal lags. Hence, the power spectral densities have continuous spectral spreads from $-\infty$ to $+\infty$. The variances of the random disturbances can be calculated by integration of the spectrum over time-infinite limits. However, because of instrument limits in time and space, and because of the conditions of field experiments, only a finite band of frequencies and a finite band of wavenumbers are actually measured. Thus only a portion of each variance of a random disturbing field appears in the averaging process. An important problem of analysis centers on determination of the effective frequency and wavenumber bands. We discuss this next.

Two choices of Fourier space are in common use. In the first the Fourier pairs are (k, x) and (ω, t), and in the second the pairs are (λ^{-1}, x) and (f, t). To illustrate, choose a function $\theta(x, t)$ which is one dimensional in space and which varies with time. Give it the dimension of temperature, °C. Then

$$S_\theta(k, \omega) = \int\int \theta(x, t) e^{i\omega t - ikx} \frac{dtdx}{(2\pi)^2} \qquad \text{(units: °C} \cdot \text{m} \cdot \text{s)}$$

and

$$S_\theta(\lambda^{-1}, f) = \int\int \theta(x, t) e^{i2\pi ft - i2\pi\lambda^{-1}x}\, dtdx \qquad \text{(units: °C} \cdot \text{m} \cdot \text{s).}$$

Let us use (λ^{-1}, f) space to illustrate a first instrument limit on the spectrum. Consider one coordinate at a time:

$$S_\theta(f) = \int S_\theta(\lambda^{-1}, f) d\lambda^{-1} = \int \theta(t) e^{i2\pi ft}\, dt.$$

Suppose $\theta(t)$ is sampled at intervals Δ_t; then the modulated signal is

$$\theta_i(t) = \theta(t) \sum_{-\infty}^{\infty} \delta(t - n\Delta_t)$$

and

$$S_i(f) = \frac{1}{\Delta_t} \sum_{-\infty}^{\infty} S_\theta\left(f - \frac{m}{\Delta_t}\right).$$

Thus the sampled time signal has a transform with period $1/\Delta_t$; that is, the Fourier transform repeats itself indefinitely. If the frequency spread of the continuous $S_\theta(f)$ overlaps the period, then frequency components $S(f)$ for $f \geq \frac{1}{2\Delta_t}$ appear in adjacent spectra. Thus the limiting f for complete recovery of $\theta(t)$ is

$$f_N = \frac{1}{2\Delta_t} \qquad \text{(units: cycle/s).}$$

This is the Nyquist limiting frequency. In a similar way, for the spatial function $\theta(x)$ sampled at intervals $1/2\ \Delta_s$, the spectrum is cut off at

$$\lambda_N^{-1} = \frac{1}{2\Delta_s} \qquad \text{(units: cycle/m).}$$

The Nyquist limits in $(k - \omega)$ space are

$$\omega_N = 2\pi f_N = 2\pi \times \frac{1}{2\Delta_t} = \frac{\pi}{\Delta_t} \qquad \text{(units: rad/s)}$$

and

$$k_N = 2\pi\lambda_N^{-1} = 2\pi \times \frac{1}{2\Delta_s} = \frac{\pi}{\Delta_s} \qquad \text{(units: rad/m)}.$$

If the measurement instrument samples time and space continuously, the Nyquist limits are infinite in all cases.

The Nyquist limit refers to sampling the spatial and temporal record of the environmental field either during the experiment or during the signal processing. We discuss next other instrument and experiment windows.

$\alpha - \omega$ Power Spectrum and Cutoffs

It was noted earlier in this report that Rayleigh's theorem allows us to write the total energy in a system over real coordinates as the integral of the absolute value squared of the spectrum of the system over all spectral components. Applying this to the selected case of a fluctuating temperature field, we note that the total energy so calculated is the variance of the fluctuating field. However, because of the nature of the measurement procedure only a portion of this variance is actually picked up by the receiver. This portion is enclosed within the bounds of the various cutoff frequencies and cutoff wavenumbers. Figure 1 shows this schematically.

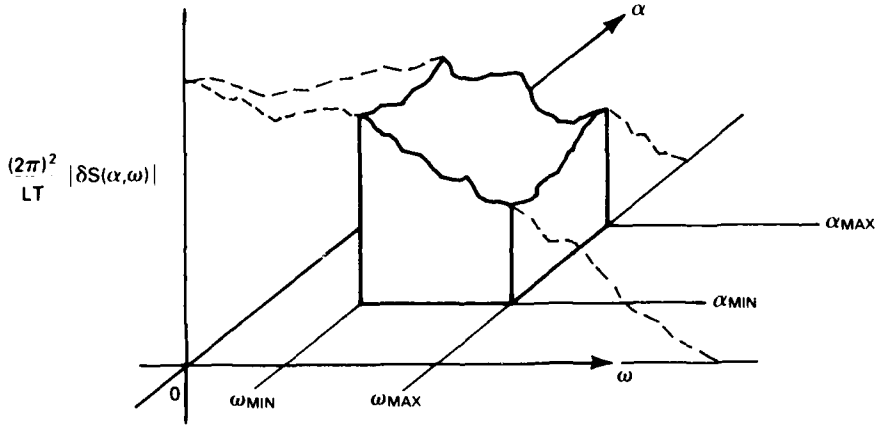

Fig. 1 — Schematic representation of cutoffs in $\alpha - \omega$ space

As noted earlier, the band-limited variance is given by

$$<\delta\theta^2(\Delta\alpha, \Delta\omega)> = \int_{\Delta\alpha}\int_{\Delta\omega} \frac{(2\pi)^2}{LT} |\delta S_{d\theta}(\alpha, \omega)|^2 \, d\alpha d\omega,$$

where

$$\delta S_{\delta\theta}(\alpha, \omega) = \frac{1}{(2\pi)^2} \int\int_{-\infty}^{\infty} \delta\theta(x, t) e^{i\omega t - i\alpha x} \, dt dx.$$

We consider the cutoff frequencies of the fluctuating temperature field $\delta\theta(x, t)$ first. Assume that the sensor is a spatial point. The field $\delta\theta(x_0, t)$ can then be decomposed into its ω-spectral components. Let the receiver have a finite response time ΔT_r. Since $\delta\theta(t)$ is a random process, some portion of it

will generally have temporal excursions which are shorter in duration than ΔT_r. The sensor will not respond to them. Thus, the spectrum of $\delta\theta$ will be cut off at a frequency ω_{max} such that

$$\omega_{max} \approx \frac{1}{\Delta T_r}.$$

Frequencies higher than ω_{max} will not *effectively* contribute energy to the receiver. Of the remaining band 0 to ω_{max}, a second portion will be cut off by the integration time ΔT_i allowed for the receiver to measure the field. This time is purposely limited to permit a high rate of data collection and to prevent the random field $\delta\theta$ from drifting into nonstationarity. The cutoff at the low frequency end is then estimated to be

$$\omega_{min} \approx \frac{1}{\Delta T_i}.$$

Between the two cutoffs one then finds the *effective* frequency band of the ω spectrum,

$$\Delta\omega = \omega_{max} - \omega_{min} = \frac{1}{\Delta T_r} - \frac{1}{\Delta T_i}, \quad \Delta T_r < \Delta T_i.$$

In towed systems the upper frequency cutoff of the internal wave spectrum may be controlled by the speed of tow. This is discussed later.

We next turn to the determination of the cutoff wavenumbers. Assume that the receiver is a linear array of $N + 1$ point sensors with uniform separation l_A. Let the total length of the array be $L_A = Nl_A$. We fix time at some instant and decompose the spatially fluctuating field $\delta\theta(x)$ into a spatial spectrum. In accordance with the Nyquist limit, all spatial periodicities less than $2l_A$ will not be effectively measured. The distance $2l_A$ is thus the minimum distance of response to the spatially fluctuating field. The upper cutoff wavenumber is, therefore,

$$\alpha_{max} \approx \frac{1}{2l_A} \qquad \text{(units: rad/m)}.$$

Of the remaining wavenumber band, 0 to α_{max}, a second portion is cut off by the length of the total field sensed L_A (i.e., track length), and

$$\alpha_{min} \approx \frac{1}{L_A} \qquad \text{(units: rad/m)}.$$

Between the two cutoffs one then finds the effective wavenumber band of the spectrum to be

$$\Delta\alpha = \alpha_{min} - \alpha_{max} = \frac{1}{2l_A} - \frac{1}{L_A} \qquad \text{(units: rad/m)}.$$

If the array is continuous rather than a collection of point sensors, the band is

$$\Delta\alpha = \infty - \frac{1}{L_A} \qquad \text{(units: rad/m)}.$$

Instrument windows have their own spatial and temporal spectra. Let $w(x,t)$ be the window modeled as the impulse response of a filter. The filter transfer function is then

$$W(\alpha, \omega) = \int w(x, t) e^{i\omega t - i\alpha x} \frac{dt d\alpha}{(2\pi)^2}.$$

The variance of a random scalar field (say temperature) is then given by

$$\langle \delta\theta^2 \rangle = \int\int_{-\infty}^{\infty} \frac{(2\pi)^2}{LT} |\delta S_{\delta\theta}(\alpha, \omega)|^2 \, |W(\alpha, \omega)|^2 \, d\alpha \, d\omega.$$

Here the spatial and temporal limits imposed by the window permit the integration limits to be $\pm\infty$. The window effectively cuts off the contributions of the $\alpha-\omega$ spectrum of the fluctuating field when these extend beyond its own limits.

Closed Form Solutions for Mean-Square Temperature Fluctuation

For the remainder of this report we consider in detail solutions of the basic equations for band-limited mean-square temperature fluctuations in the ocean. It was noted earlier that for a Gaussian autocorrelation of the temperature field $\theta(x,t)$ the band-limited variance is

$$<\delta\theta^2(\Delta\alpha,\ \Delta\omega)> = \iint_{\Delta\alpha\Delta\omega} \frac{<\delta\theta^2>\, l_{c\theta}\tau_{c\theta}}{2\pi}\, e^{-\frac{\omega^2\tau_{c\theta}^2}{2}}\, e^{-\frac{\alpha^2 l_{c\theta}^2}{2}}\, d\alpha\, d\omega \quad \text{(units: } (^\circ\text{C})^2\text{)}.$$

The integration is elementary if the assumption is made that there is no dispersion:

$$<\delta\theta^2(\Delta\alpha,\ \Delta\omega)> = \frac{<\delta\theta^2>}{4}\left[\operatorname{erf}\left(\frac{\alpha_{\max} l_{c\theta}}{\sqrt{2}}\right) - \operatorname{erf}\left(\frac{\alpha_{\min} l_{c\theta}}{\sqrt{2}}\right)\right] \times \left[\operatorname{erf}\left(\frac{\omega_{\max}\tau_{c_\theta}}{\sqrt{2}}\right) - \operatorname{erf}\left(\frac{\omega_{\min}\tau_{c\theta}}{\sqrt{2}}\right)\right],$$

where

$$\operatorname{erf}(z) = \frac{2}{\sqrt{\pi}}\int_0^z e^{-t^2}\, dt.$$

This is a closed-form solution. Here, as before, the values of $\alpha_{\max}$, $\alpha_{\min}$, $\omega_{\max}$, and $\omega_{\min}$ must be determined by considerations of the instrumental and experimental cutoffs to the $\alpha-\omega$ spectrum described earlier in this report.

We next consider a towed sensor. Let the speed of tow be v(m/s). If this is fast enough (say greater than a few knots) the ocean temperature field is essentially "frozen." Then we can convert the ω spectrum to an α spectrum by writing $\alpha = \omega/v$. For a Gaussian autocorrelation of the temperature field we find the closed form solution

$$<\delta\theta^2(\Delta\omega/v)> = \frac{<\delta\theta^2>}{2}\left[\operatorname{erf}\left(\frac{\omega_{\max} l_{c\theta}}{\sqrt{2}v}\right) - \operatorname{erf}\left(\frac{\omega_{\min} l_{c\theta}}{\sqrt{2}v}\right)\right].$$

These band-limited variances of the temperature field will be used later in making numerical estimates. This completes the first major portion of our investigation.

We now take up the second major problem, which is to make numerical estimates of the effects of temperature fluctuations on the phase stability of optical-fiber hydrophones.

TEMPERATURE FIELDS IN THE OCEAN

The temperature field $\theta(\mathbf{r},t)$ in the ocean is a complex phenomenon. It consists of several component fields distinguished among themselves by differing length and time scales. First, there is a long-duration mean-temperature variation with range and depth, labeled the temperature profile. Secondly, there is a faster space-time fluctuation of temperature at each range and depth about the mean profile. Thirdly, there is a still shorter scale space- and time-varying microstructure of temperature which also varies with range and depth. The causes of these component phenomena are thought to be seasonal solar heating which forms the profiles; internal waves generated by winds, convection currents, etc. which distort the profiles in space and time; and velocity turbulence and thermal diffusion, which are responsible for creating the temperature microstructure.

We concentrate here first on the fluctuations in temperature profile caused by internal waves and second on the temperature microstructure. Our objective is to calculate band-limited variances of temperature fluctuation in each category and from these to calculate the mean-square fluctuation in phase of a laser light beam being transmitted through a fiber submerged in the random temperature field.

We begin with the effect of internal waves on the temperature field. Before entering the analysis, we define the concept of one-dimensional spectra, which are the major tools for calculation.

One-Dimensional Spectra

All spectra used in this report are one dimensional. They are derived from three- or four-dimensional spectra by integration in the usual way. Let

$$<\delta\theta(\mathbf{x},t)\,\delta\theta(\mathbf{x}+\boldsymbol{\xi},\,t+\tau)> = <\delta\theta^2>\,\rho(\boldsymbol{\xi},\tau)$$
$$=\int_{-\infty}^{\infty} e^{i\boldsymbol{\alpha}\cdot\boldsymbol{\xi}\;-\;i\omega\tau}\,\delta S_\theta(\boldsymbol{\alpha},\omega)\,d\boldsymbol{\alpha}\,d\omega,$$

where ρ is the nondimensional correlation function and δS is the spectral density. Then the one-dimensional spectra are generated as follows:

$$<\delta\theta^2>\,\rho(\alpha_1,\,0,\,0,\,0) = \int_{-\infty}^{\infty} e^{i\xi\alpha_1}\,\delta S_\theta(\boldsymbol{\alpha},\,\omega)\,d\boldsymbol{\alpha}\,d\omega \tag{1}$$
$$= \int_{-\infty}^{\infty} e^{i\xi_1\alpha_1}\left(\int\int\int_{-\infty}^{\infty}\delta S_\theta(\boldsymbol{\alpha},\,\omega)\,d\alpha_2 d\alpha_3 d\omega\right) d\alpha_1$$
$$= \int_{-\infty}^{\infty} e^{i\xi_1\alpha_1}\,F^1(\alpha_1)\,d\alpha_1,$$

where $F^1(\alpha_1)$ is the one-dimensional spectral density along coordinate ξ_1, and

$$<\delta\theta^2> = \rho(0,\,0,\,0,\,\omega) = \int_{-\infty}^{\infty} e^{-i\omega\tau}\,F^4(\omega)\,d\omega, \tag{2}$$
$$F^4(\omega) = \int\int\int_{-\infty}^{\infty} e^{i\boldsymbol{\alpha}\cdot\boldsymbol{\xi}}\,\delta S(\boldsymbol{\alpha},\,\omega)\,d\boldsymbol{\alpha},$$

where $F^4(\omega)$ is the one-dimensional spectral density along the coordinate of time. If the field $\delta\theta$ is isotropic in space, then

$$\delta S(\boldsymbol{\alpha},\omega) = \delta S(\alpha,\omega),\quad \alpha^2 = \boldsymbol{\alpha}\cdot\boldsymbol{\alpha}.$$

If the field is not isotropic, it is sometimes convenient to define a three-dimensional spectrum of a single variable by integration over a spherical shell of radius α:

$$E(\alpha,\omega) = \int\int_{\boldsymbol{\alpha}\cdot\boldsymbol{\alpha}=\alpha^2}\delta S(\boldsymbol{\alpha},\omega)\,dA.$$

Then

$$<\delta\theta^2> = \int_0^{\infty} E(\alpha)\,d\alpha.$$

Garrett and Munk Spectrum for Internal Waves

Garrett and Munk proposed a model, called GM72 [3], later improved to GM75 [6], of a power spectrum of vertical displacement of the ocean medium at various depths caused by internal waves. The model is given by their Eqs. (6.20) and (6.22):

$$\hat{n}\;\hat{F}_\zeta(\omega) = \frac{1}{2}\,\frac{1}{\pi^3}\,E\omega_i\,\frac{1}{\hat{M}^2}\,\frac{1}{\omega^3}(\omega^2-\omega_i^2)^{\frac{1}{2}} \tag{GM6.20}$$

$$\hat{n}\,\hat{F}_\zeta(\alpha_1) \cong \frac{j_*}{2}\,\frac{1}{\pi^3}\,E\omega_*\,\frac{1}{\hat{M}^3}\,\hat{N}\,\frac{1}{\alpha_1^2}, \qquad \omega_* << \omega_\mu << n. \tag{GM6.22}$$

The symbols used by them are very special. They are listed in Table 1 together with their units.

Table 1—Garrett and Munk Symbols

Symbol*	Meaning	SI Units	GM Physical Units
$\hat{n}$	Vaisala frequency	s^{-1}	cph
$F_\zeta(\omega)$	vertical displacement ω spectrum	$m^2 \cdot s$	m^2/cph
E	nondimensional energy		
ω_*	nondimensional inertial frequency		
$\hat{M}$	scale factor for spatial coordinates	m^{-1}	cpkm
ω	nondimensional frequency		
$\hat{F}_\zeta(\alpha_1)$	vertical displacement α spectrum	m^3	$m^2 \cdot$ cycle/m
$\hat{N}$	scale factor for time coordinate	s^{-1}	cph
α_1	nondimensional wavenumber		
$\hat{\alpha}$	wavenumber	m^{-1}	cpm
$\hat{\omega}_*$	inertial frequency	s^{-1}	cph
$\hat{E}$	energy in units of velocity^2 × distance	$m^3 \cdot s^{-2}$	
$\hat{\rho}$	mass density	$N \cdot s^2 \cdot m^{-4}$	
$\hat{\rho}\hat{E}$	energy per unit area	$N \cdot m/m^2$	J/cm^2
$\hat{E}(y)$	energy in units of velocity^2	$m^2 \cdot s^{-2}$	
$\hat{\rho}E(y)$	energy per unit volume	$N \cdot m/m^3$	J/cm^3
x, y	range, depth	m	
$\hat{b}$	$\frac{1}{2\pi\hat{M}}$ buoyancy depth scale	m	m/rad

*Also, $\alpha = \hat{\alpha}/\hat{M}$, $\omega = \hat{\omega}/\hat{N}$, $n = \hat{n}/\hat{N}$, $x = 2\pi\hat{M}\hat{x}$, $t = 2\pi\hat{N}\hat{t}$, and an exponential model of $\hat{n}$ is given by $\hat{n} = \hat{N}e^{-\hat{y}/\hat{b}}$, where $\hat{b} = 1.3$ km and $\hat{y} > 200$m.

By curve-fitting to ocean data GM72 assigned the following values:

$$\hat{M} = 0.122\,\text{cycles/km} = 1.22 \times 10^{-6}\,\text{cycles/cm} = 1.22 \times 10^{-4}\,\text{cycles/m},$$
$$\hat{M}^{-1} = 8.196 \times 10^5\,\text{cm/cycle} = 8.196 \times 10^3\,\text{m/cycle},$$
$$\hat{N} = 3\,\text{cycles/h} = 8.333 \times 10^{-4}\,\text{cycles/s}.$$
$$\hat{M}^{-3}\hat{N}^2 = (8.196 \times 10^5)^3\,(8.333 \times 10^{-4})^2 = 3.824 \times 10^{11}\,\text{cm}^3/\text{s}^2,$$
$$\hat{E} = 3.82 \times 10^6\,\text{cm}^3/\text{s}^2,$$
$$\hat{\rho}\hat{E} = 0.382\,\text{J/cm}^2 = 3.82 \times 10^6\,\text{erg/cm}^2,$$
$$\hat{\rho} = 1\,\text{g/cm}^3 = 1\,\text{dyne} \cdot \text{s}^2/\text{cm}^4\ (1\,\text{kN} \cdot \text{s}^2/\text{m}^4),$$
$$E = \frac{\hat{E}}{\hat{M}^{-2}N^2\hat{b}} = \frac{\hat{E}2\pi}{\hat{M}^{-3}N^2} = \frac{3.82 \times 10^6 \times 2\pi}{3.82 \times 10^{11}} = 2\pi \times 10^{-5},$$
$$\hat{\omega}_* = 0.04\,\text{cph} = 1.111 \times 10^{-5}\,\text{cycle/s (at } 30^\circ\text{ lat.)},$$
$$j_* = j_k = 20\text{ modes, and}$$
$$\hat{b} = 1.3\,\text{km} = 1.3 \times 10^3\,\text{m} = 1.3 \times 10^5\,\text{cm}.$$

In order to obtain a quantitative feeling of these entities we cite a few examples.

Example 1: In Fig. 2 (GM72 [3] Fig. 4) choose $\hat{\alpha}_1 = 1$ cpkm (cycle per kilometer), then

$$\alpha_1 = \frac{\hat{\alpha}_1}{\hat{M}} = \frac{1\,\text{cpkm}}{0.122\,\text{cpkm}} = 8.196$$

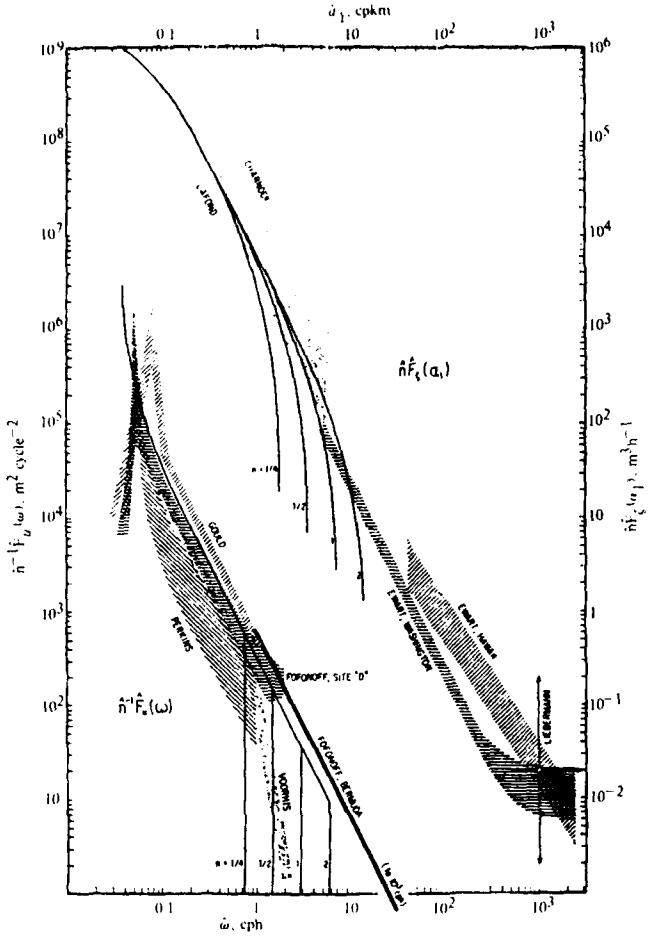

Fig. 2 — Garrett and Munk spectra of vertical wave displacement due to internal waves. Bands represent the observed moored and floating spectra (left) and towed spectra (right). Dotted bands are presumably not subject to fine-structure noise. Curves are the derived relations (6.20, 21). (GM72 [3], Fig. 4).

and

$$\omega_i = \frac{\hat{\omega}_i}{\hat{N}} = \frac{0.04\text{cph}}{3\text{cph}} = 1.333 \times 10^{-2}.$$

Thus,

$$\hat{n}\hat{F}_\zeta(\alpha_1) = \left(\frac{20}{2}\frac{1}{\pi^3}\, 2\pi \times 10^{-5}\right)(0.04\text{ cph}) \times (8.196\times 10^3)^3 \left(\frac{1}{(8.196)^2}\right)$$

$$= 6.64 \times 10^3\ \text{m}^3/\text{h}.$$

This checks with the value in Fig. 2.

Example 2: At depth $\hat{y} = 300$ m, from the GM72 exponential model of the Vaisala frequency

$$\hat{n} = \hat{N}\exp(-\hat{y}/\hat{b});\quad \hat{N} = \hat{n}(\hat{y}=0) = \hat{n}_0 = 3\text{ cph},$$

$$= 3\text{cph} \times \exp\left(-\frac{300}{1300}\right) = 2.38\text{ cph},$$

and

$$\hat{F}_\zeta(\alpha_1) = \frac{6.64\times 10^3\ \mathrm{m^3/h}}{2.38\ \mathrm{cph}} = 2.79\times 10^3 \frac{\mathrm{m^3}}{\mathrm{cycle}} \left[or\ \frac{\mathrm{m^2}}{\mathrm{cpm}}\right].$$

This also checks with the value found in Fig. 2.

Example 3: According to GM72 Eq. (6.20),

$$\hat{n}^{-1}\hat{F}_u(\omega) = \frac{2}{\pi} E\omega_i \hat{M}^{-2}\omega^{-3}\left[\frac{\omega^2+\omega_i^2}{\sqrt{\omega^2-\omega_i^2}}\right] \quad \left[\text{units: } \frac{\mathrm{m^2}}{\mathrm{cycle^2}}\right].$$

Now choose $\hat{\omega} = 0.1$ cph,

$$\omega = \frac{\hat{\omega}}{\hat{N}} = \frac{0.1\ \mathrm{cph}}{3\ \mathrm{cph}} = 3.333\times 10^{-2}$$

and

$$\omega_i = \frac{\hat{\omega}_i}{\hat{N}} = \frac{0.04\ \mathrm{cph}}{3\ \mathrm{cph}} = 1.333\times 10^{-2}.$$

Thus,

$$\hat{n}^{-1}\hat{F}_u(\omega) = \frac{2}{\pi} \times \frac{(2\pi\times 10^{-5})(1.333\times 10^{-2})\ (8.196\times 10^3)^2}{(3.333\times 10^{-2})^3} \times \left[\frac{(3.333\times 10^{-2})^2 + (1.333\times 10^{-2})^2}{\sqrt{(3.333\times 10^{-2})^2 - (1.333\times 10^{-2})^2}}\right]$$

$$= 4.08\times 10^4\ \mathrm{m^2/cycle^2}.$$

This checks with the value shown in Fig. 2.

The proposed GM72 model also gives a relation between vertical displacement spectra and vertical velocity spectra:

$$\frac{\hat{n}^{-1}\hat{F}_u(\omega)}{\hat{n}\,\hat{F}_\zeta(\omega)} = 4\pi^2\,\frac{\omega^2+\omega_i^2}{\omega^2-\omega_i^2}.$$

Thus, if $\omega^2 >> \omega_i^2$, then

$$\hat{n}^{-1}\hat{F}_u(\omega) \rightarrow \hat{n}\,\hat{F}_\zeta(\omega)\,4\pi^2$$

or

$$\hat{F}_u(\omega) \rightarrow \hat{n}^2\hat{F}_\zeta(\omega)\,4\pi^2 \quad \left[\text{units: } \frac{\mathrm{m^2}}{\mathrm{h^2}}\frac{1}{\mathrm{cph}}\right].$$

One can then find $\hat{F}_u(\omega)$, if convenient, then obtain $\hat{F}_\zeta(\omega)$.

Ocean Vertical Displacement Spectra

Power spectra of internal waves are classified by GM72 according to the method of measurement: towed spectra (TS), obtained by towing temperature-sensitive sensors along a horizonal line in the ocean; moored spectra (MS), obtained by fixing the sensors in a location in the ocean; or dropped spectra (DS), obtained by dropping weighted sensors in the ocean. In each case the Garrett and Munk

models of spectra in the three spectral coordinates (horizontal wavenumber α_1, vertical wavenumber α_2, and frequency ω) are collapsed by integration into a single coordinate. The selected single coordinates are α_1, in TS; ω, in MS; and α_2, in DS. Examples of spectra used in this report are found in GM72 [3] and GM75 [6]. Figures 3a, 3b, and 3c reproduce Figs. 2, 3, and 5 of GM75.

In each of these experimentally obtained spectra the corresponding models of GM72 and GM75 are superimposed. Of particular importance are the upper limits of measurement: $\alpha_1 \approx 3 \times 10^{-2}$ cycle/m in TS, $\omega \approx 8$ cycle/h in MS, and $\beta n_0/n \approx 30$ cycle/m in DS; and the lower limits of measurement: $\alpha_1 \approx 3 \times 10^{-5}$ cycle/m in TS, $\omega \approx 10^{-1}$ cycle/h in MS, and $\beta n_0/n \approx 3 \times 10^{-2}$ cycle/m in DS. These limits impose restrictions on the possible cutoffs in the calculation of band-limited variances undertaken later in this report.

Figure 3a (GM75 Fig. 2) also shows a spectrum of moored vertical coherence (MVC). This report does not discuss explicitly coherence and its effect on noise calculations. We intend to investigate these effects in subsequent reports.

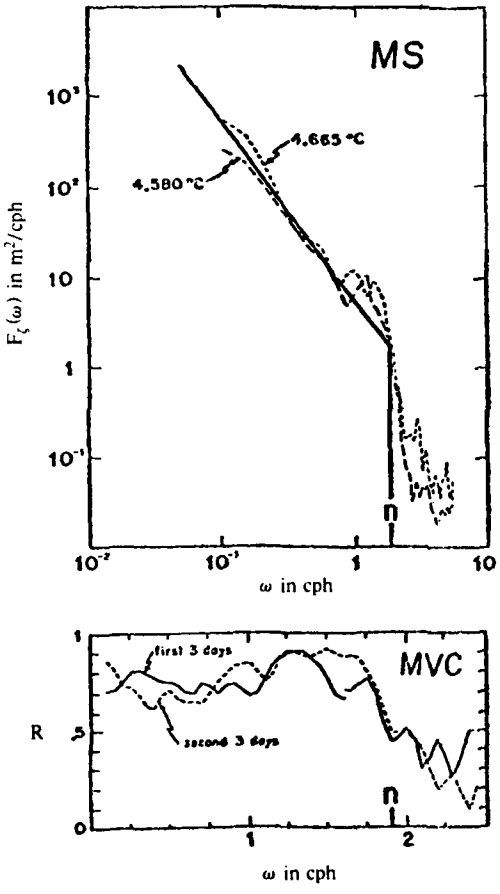

Fig. 3a — Moored spectrum in coordinate ω obtained by J.L. Cairns [J. Geophys. Res. 80, 299-306 (1975)] (GM75 [6], Fig. 2)

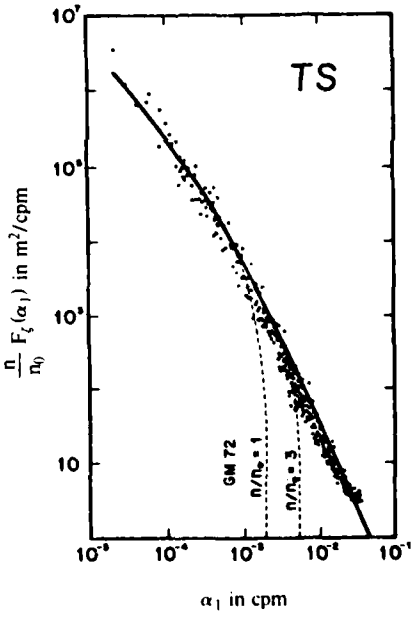

Fig. 3b — Improved normalized towed spectrum in coordinate α_1 made by E.J. Katz [J. Phys. Oceanogr. 3, 448-457 (1973)] (GM75 [6], Fig. 3)

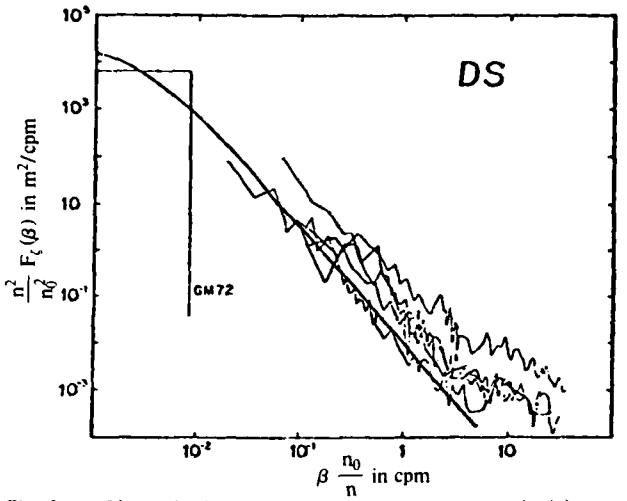

Fig. 3c — Normalized dropped spectrum in coordinate $(n_0/n)\beta = (n_0/n)\alpha_2$ obtained by R. Millard [MODE Hot Line News, No. 18, 1 (1972)] (GM75 [6], Fig. 5)

Effects of Tow Speed on the Spectrum

The α_1, α_2, ω spectrum of vertical displacement of internal waves describes both spatial and temporal aspects of the vertical displacement as natural phenomena of the ocean. In contrast, the speed of tow describes how fast the phenomena are sampled in time. At "infinite" speed the sampling is instantaneous. Hence the resulting spectrum is that of a "frozen ocean." It is a wavenumber spectrum. At zero speed of tow the sampling in spatial terms vanishes, leaving only a sampling in time. The data contribute only to a frequency spectrum. The model of these spectra used in this report is that of Garrett and Munk, GM72. This model specifies the zero-speed spectrum as the *moored spectrum* (MS) and the infinite-speed spectrum as the *towed spectrum* (TS). At intermediate tow speeds the sampling time is slow enough to permit the ocean to vary somewhat in time during sampling. GM72 models these intermediate speeds in Fig. 9 of their article, reproduced here as Fig. 4. At low speeds the spectra are plotted as $\hat{n}\hat{F}_\zeta(\sigma)$ vs σ, where $\sigma = |\omega - \alpha S|$ is the "frequency of encounter." They are essentially modified *moored spectra*. At high speeds the spectra are plotted as $\hat{n}\hat{S}\hat{F}_\zeta(\alpha_1)$ vs $\hat{\sigma}/\hat{S}$. They are essentially wavenumber spectra which merge into the GM72 model of *towed spectra* when the speed is infinite. Figure 4 (GM72 Fig.9) also shows that intermediate speeds strongly affect only the upper and lower limits of the spectra. The influence of tow speed on the middle ranges of the spectra is minimal. Thus, for ordinary tow speeds (say 2 knots and above) the ocean is essentially frozen for internal waves, except for the very shortest and very longest wavelengths. However, actual experimental data (see Fig. 2 [Fig. 4 of GM72]) do not agree with the model at the upper and lower extremities of the spectra. These discrepancies have been removed in a later model, GM75 [6]. The calculations of this report are unaffected by them, since they are based on the middle ranges of the spectra, the model of which is not changed in GM75.

Calculation of the Mean-Square Fluctuation in Temperature over a Towed Fiber

A fiber of length $L = 1000$ m is towed at a depth of $\hat{y} = 100$ m at a speed S knots such that it floats horizontally. We wish to calculate the mean-square fluctuation in temperature $<\delta\theta^2>$ over the entire length for all temporal frequencies and vertical wavenumbers.

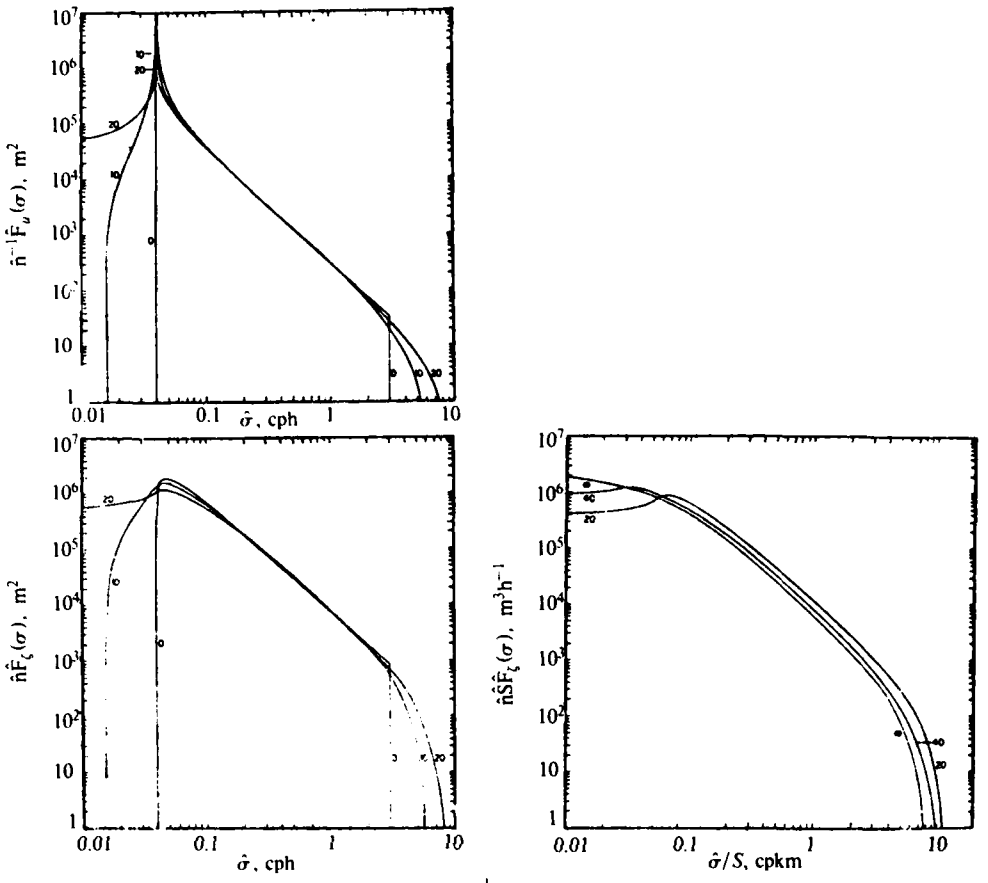

Fig. 4 — Doppler effects on the current spectrum (left) and vertical displacement spectrum (below), for $n = 1$ (3 cph), $E = 2\pi \times 10^{-5}$ (0.38 joules/cm²), $j_i = 20$. For low speeds the spectra are plotted against frequency-of-encounter $\hat{\sigma}$; for high speeds, against $\hat{\sigma}/\hat{S}$. The curves are for relative speeds $\hat{S}/\hat{S}_0 = 0, 0.45, 0.90, 1.80, \infty$ ($\hat{S} = 0, 10, 20, 40, \infty$ cm/sec) with 0, ∞ corresponding to the moored and towed spectra (6.20, 6.21) respectively. (GM72 [3], Fig. 9)

To make this calculation we shall use the convenient formula [3, footnote on page 237]:

$$<\delta\theta^2(\Delta\alpha_1, \hat{y})> = \left(\frac{dT}{d\hat{y}}\right)^2 \int_{\Delta\hat{\alpha}_1} \hat{F}_\zeta\ (\alpha_1, \hat{y})\, d\hat{\alpha}_1 = \left(\frac{dT}{d\hat{y}}\right)^2 <\zeta^2>.$$

Thus, we must first find the mean-square vertical displacement $<\zeta^2>$ and the temperature gradient $dT/d\hat{y}$ at the depth $\hat{y}$ in question. To do this we require ocean data and a suitable model of the power spectrum $F_\zeta(\alpha_1, \hat{y})$. A well-substantiated model has been proposed in several articles by Garrett and Munk [3,6]. We assume in what follows that $\hat{F}_\zeta(\alpha_1)$ is the same as in GM72 [3] Eq. (6.22). This is called by them the *towed spectrum*, and is a model developed from the data of many towed sensor experiments. It includes the effects of all temporal frequencies and all vertical wavenumbers associated with internal waves. A more elaborate model of towed spectra is found in Fig. 4 (Fig. 9 of GM72). It shows that the parameter S (tow speed) affects the spectrum appreciably only at the upper and lower ends and very little over most of the portion in between. We shall use here only the simplest GM72 version of the tow spectrum, which has the form

$$\hat{F}_\zeta\ (\alpha_1) \approx \frac{1}{\hat{n}}\ \frac{1}{2}\ j_i\ \frac{1}{\pi^3}\ \frac{E\,\omega_i\,N}{\hat{M}^3\alpha_1^2}, \qquad \omega_i < \omega_\mu < n.$$

The definitions and values assigned to the symbols are taken from GM72 [3] and Bell et al. [7]:

$\hat{n}$ = Vaisala frequency—at 100 m, $\hat{n} = 5.0$ cycle/h;
j_i = number of vertical modes—GM72 takes $j_i = 20$;
E = dimensionless energy constant—GM72 assigns $E = 2\pi \times 10^{-5}$;
ω_i = dimensionless inertial frequency—GM72 assigns

$$\omega_i = \frac{\hat{\omega}_i}{\hat{N}} = \frac{0.04\,\text{cph}}{3\,\text{cph}} = 1.333 \times 10^{-2};$$

$\frac{dT}{d\hat{y}}$ = temperature gradient at depth $\hat{y}$
≈ 0.025 at 100-m depth (a discussion of temperature gradient is undertaken in the next section of this report);
$\hat{M}$ = spatial scale factor—GM72 assigns $\hat{M} = 0.122$ cycle/km;
$\hat{N}$ = temporal scale factor—GM72 assigns $\hat{N} = 3$ cycle/h;
α_1 = dimensionless wavenumber—GM72 assigns

$$\alpha_1 = \frac{\hat{\alpha}_1}{\hat{M}} = \frac{\hat{\alpha}_1}{0.122} = 8.196\hat{\alpha}_1 ,$$

where $\hat{\alpha}_1$ is the wavenumber in units of cycle/km.

We calculate the constant factors of F_ζ in units of meters and hours:

$$\frac{1}{\hat{n}} \frac{1}{2} j_i \frac{1}{\pi^3} \frac{E\omega_i N}{\hat{M}^3} = \frac{1}{5.0} \times \frac{1}{2} \times 20 \frac{1}{\pi^3} \times \frac{2\pi \times 10^{-5} \times 1.333 \times 10^{-2} \times 3}{(1.22 \times 10^{-4})^3}$$

$$= 8.925 \times 10^4 \text{ m}^3/\text{cycle } (=\text{m}^2/\text{cpm}).$$

The integral required is

$$I = \int_{\Delta\alpha} \frac{d\hat{\alpha}_1}{\alpha_1^2} = \hat{M}^2 \int \frac{d\hat{\alpha}_1}{\hat{\alpha}_1^2} = \hat{M}^2 \left[-\left[\frac{1}{\hat{\alpha}_{1\max}} - \frac{1}{\hat{\alpha}_{1\min}} \right] \right].$$

Since the upper portions of the spectrum contain little energy, we arbitrarily take $\hat{\alpha}_{1\max} \to \infty$. The minimum wavenumber must be estimated. If we assume slow tow, and the effective length of the data sample is 1000 m, we estimate

$$\hat{\alpha}_{1\min} \approx \frac{1\text{cycle}}{1000\text{m}} = 10^{-3} \text{ cpm}.$$

Thus,

$$I \approx (1.22 \times 10^{-4})^2 \times \frac{1}{10^{-3}} = 1.488 \times 10^{-5} \text{ cpm}$$

and

$$\langle \zeta^2 \rangle = \int \hat{F}_\zeta (\alpha_1) d\hat{\alpha}_1 = 8.925 \times 10^4 \frac{\text{m}^2}{\text{cpm}} \times 1.488 \times 10^{-5} \text{ cpm}$$

$$= 1.33 \text{ m}^2.$$

This means that over a length of 1000 m the rms vertical displacement at a depth of 100 m is about 1 m. The rms temperature fluctuation over the length of the fiber is thus

$$\langle \delta\theta^2(\Delta\alpha, \hat{y}) \rangle = (0.025)^2 \times 1.33 = 8.3 \times 10^{-4} \text{ (°C)}^2.$$

Note that this result *includes* the effect of *all* frequencies [6].

Discussion: Clearly at a different depth both the Vaisala frequency and the temperature gradient will be different from what is assumed above. Thus the calculation will be strongly depth dependent. Also it must be recognized that GM72 does not give a good approximation if the tow depth is less than 100 m. In these shallow depths the mixing of different temperature strata partially destroys the internal wave structure.

To check our result, we asked: What will be the value of $<\zeta^2>$ if the *entire* spectrum of energy is considered? To answer this we made the following calculation.

Let us consider the case of towed spectra given by Fig. 5 (Fig. 1 of Bell et al. [7]). We can approximate the function $\hat{F}_\zeta(\alpha_1)$ (units: m^2/cpm) by the formula

$$\hat{F}_\zeta(\alpha_1) = 10^5 \left(\frac{\hat{\alpha}_1}{10^{-4}}\right)^{-2} = \frac{10^5 \times 10^{-8}}{\hat{\alpha}_1^2} = \frac{10^{-3}}{\hat{\alpha}_1^2},$$

in which the units of $\hat{\alpha}_1$ are cpm. To check, take $\hat{\alpha}_1 = 10^{-3}$ cpm; then $\hat{F}_\zeta \approx 10^3$, which agrees with Fig. 5 (Fig. 1 of [7]). Now

$$<\zeta^2> = \int \hat{F}_\zeta(\alpha_1)\, d\hat{\alpha}_1 = 10^{-3} \int \frac{d\hat{\alpha}_1}{\hat{\alpha}_1^2} = 10^{-3}\left[-\left[\frac{1}{\hat{\alpha}_{1\max}} - \frac{1}{\alpha_{1\min}}\right]\right].$$

Choose $\alpha_{1\max} \to \infty$; then

$$I = 10^{-3}\left(\frac{1}{\alpha_{1\min}}\right).$$

Assume $\alpha_{1\min} \approx 10^{-4}$ cpm; then

$$<\zeta^2> = 10\,m^2 \text{ and } \sqrt{<\zeta^2>} = 3m.$$

For the range shown in Fig. 5 (Fig. 1 of [7]),

$$<\zeta^2> = 10^{-3}\left(\frac{1}{10^{-4}} - \frac{1}{10^{-2}}\right) \approx 10\,m^2.$$

Thus at a depth of 100 m, a towed sensor will show a root-mean-square value of vertical displacement of about 3 m when *all* wavenumbers from 10^{-4} to ∞ cpm are considered. In the earlier calculation we considered the spectrum contributions at the lower end to stop at 10^{-3} cpm, which gave the result $<\zeta^2> \approx 1.33\ m^2$. The corresponding temperature fluctuation for the entire spectrum is $<\delta\theta^2> = 6.2 \times 10^{-3}\ (°C)^2$. Note again that the spectrum $\hat{F}_\zeta(\alpha_1)$ includes the effect of *all* frequencies, as required both by definition and construction.

Calculation of Phase Fluctuations Caused by Temperature Fluctuations

We noted in the section "Environmental Noise" that the phase fluctuation $\delta\phi$ due to temperature fluctuation $\delta\theta(x)$ with correlation length L_c in a fiber of length L, of index of refraction n, transmitting a laser light of wavelength λ_0, is

$$\sqrt{<\delta\phi_L^2>} = C_{\theta L}\sqrt{2LL_c<\delta\theta^2>}.$$

Assuming that $2LL_c = O(1)\ m^2$ and using the explicit form of $C_{\theta L}$, we write

$$\sqrt{<\delta\phi_L^2>} = k_0 n\left(\frac{1}{n}\frac{\partial n}{\partial\theta} + \frac{1}{L}\frac{\partial L}{\partial\theta}\right)\sqrt{<\delta\theta^2>}.$$

Let us choose a glass fiber and make the additional specifications

$$n = 1.46,$$

$$\lambda_0 = 5.6 \times 10^3\ Å.$$

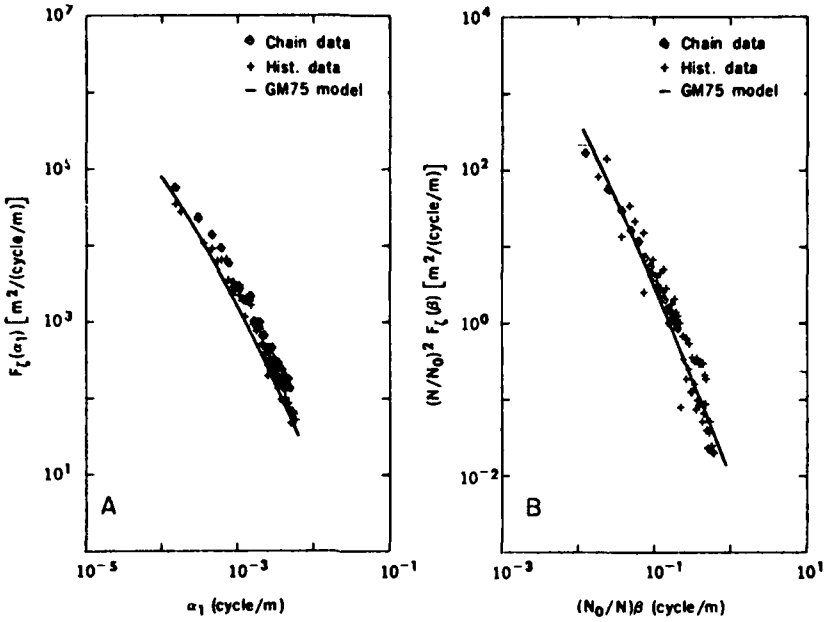

Fig. 5 — Normalized horizontal (A) and vertical (B) one-dimensional spectra of internal wave amplitude (Bell et al. [7], Fig. 1)

$$\frac{1}{L}\frac{\partial L}{\partial \theta} = 4 \times 10^{-7} \qquad \left[\text{units: } \frac{1}{\text{℃}}\right],$$

and

$$\frac{\partial n}{\partial \theta} = 11.9 \times 10^{-6} \qquad \left[\text{units: } \frac{1}{\text{℃}}\right].$$

Then

$$k_0 = \frac{2\pi}{\lambda_0} = \frac{2\pi}{5.6 \times 10^{-7}\,\text{m}} = 1.122 \times 10^7\ \text{m}^{-1},$$

and

$$k_0 n\left(\frac{1}{n}\frac{\partial n}{\partial \theta} + \frac{1}{L}\frac{\partial L}{\partial \theta}\right) = 1.122 \times 10^7 \left(\frac{11.9 \times 10^{-6}}{1.46} + 4 \times 10^{-7}\right) \times 1.46$$

$$= 1.40 \times 10^2 \qquad \left[\text{units: } \frac{\text{rad}}{\text{℃} \cdot \text{m}}\right].$$

Hence,

$$\sqrt{<\delta\phi_L^2>} = 1.40 \times 10^2 \sqrt{<\delta\theta^2>}.$$

We continue the calculation of $\sqrt{<\delta\phi_L^2>}$ using the GM72 spectrum for various fiber lengths L. The results are shown in Table 2. Actual calculations are shown in Appendix F.

Table 2—Values of $\sqrt{<\delta\phi_L^2>}$ for Various Fiber Lengths L

L (m)	$\sqrt{<\delta\phi^2>}$ (rad)
10^3	4.04
10^2	1.28
10	0.404*
1	0.128*

*Extrapolated values (uncertain)

Temperature Gradient

The temperature gradient $\partial T/\partial z$ in the ocean is a function of depth, season, salinity, etc. In any particular calculation of temperature fluctuation it is essential to measure this gradient at the locale in question. However, it is equally useful to have a model of this parameter.

A convenient starting point in the development of this model is the equation of sound speed gradient proposed by Munk [8]:

$$\frac{\partial_z C}{C} = \alpha \frac{\partial T'}{\partial z} + \beta \frac{\partial S}{\partial z} + \gamma_A,$$

where

$\alpha = 3.16 \times 10^{-3}(\text{°C})^{-1}$;

$\beta = 0.96 \times 10^{-3}(\text{‰})^{-1}$;

$\gamma_A = 1.14 \times 10^{-2}\ \text{km}^{-1}$;

$\partial_z C = \partial C/\partial z$;

$C(z)$ is the speed of sound as a function of depth;

T' is the potential temperature, which is the observed temperature minus the adiabatic gradient;

S is the salinity; and

γ_A is the fractional velocity gradient in an adiabatic ocean.

We first eliminate salinity effects by use of the *Turner number*, *Tu*:

$$\frac{\partial S}{\partial z} = \frac{a}{b} \frac{\partial T'}{\partial z} Tu.$$

Thus,

$$\frac{\partial_z C}{C} = \alpha \frac{\partial T'}{\partial z} + \frac{\beta a}{b} \frac{\partial T'}{\partial z} Tu + \gamma_A$$

and

$$\frac{\partial T'}{\partial z} = \frac{C^{-1}\partial_z C - \gamma_A}{\alpha(1 + cTu)},$$

where

$$c = \frac{a\beta}{\alpha b}.$$

The fractional sound speed gradient is related to the Vaisala frequency $N(z)$. In Munk's model,

$$C^{-1}\partial_z C = -\left(\frac{\mu}{g}\right) N^2(z) + \gamma_A,$$

$$\mu = \frac{\alpha}{a}\, s(Tu),$$

$$s(Tu) = \frac{1 + cTu}{1 - Tu},$$

$$\frac{\alpha}{a} = 24.3,$$

and

$$c = \frac{a\beta}{\alpha b} = 0.049.$$

Thus,

$$\frac{\partial T'}{\partial z} = \frac{-\left(\frac{\mu}{g}\right)N^2(z)}{\alpha(1 + cTu)} = -\frac{\alpha(1 + cTu)}{ag(1 - Tu)} \times \frac{1}{\alpha}\,\frac{N^2(z)}{(1 + cTu)}$$

$$= -\frac{N^2(z)}{ag(1 - Tu)}.$$

A convenient model of the Vaisala frequency below the thermocline is the exponential one,

$$N = N_0 e^{-z/B},$$

$$N_0 = 5.24 \times 10^{-3}\,\frac{\text{rad}}{\text{s}}\ (= 3\ \text{cph}),$$

and

$$B = 1.3\ \text{km}.$$

In the Atlantic near Bermuda Tu is about $+0.8$. Thus, with depth in meters,

$$\frac{\partial T'}{\partial z} = -\frac{(5.24 \times 10^{-3})^2 e^{-2z/1.3\times 10^3}}{1.3 \times 10^{-4} \times 9.8(1 - 0.8)} \quad (\text{units: } ^\circ\text{C/m}).$$

Hence, at $z = 100$ m,

$$\frac{\partial T'}{\partial z} = -\frac{(5.24 \times 10^{-3})^2\, e^{-\frac{2\times 10^2}{1.3\times 10^3}}}{1.3 \times 10^{-4} \times 9.8(0.2)}$$

$$= -9.3 \times 10^{-2}\ ^\circ\text{C/m}.$$

In the North Pacific $Tu \approx -0.3$. Hence at 100-m depth $\frac{\partial T'}{\partial z} = -1.4 \times 10^{-2}$ °C/m. These are average values over whole ocean basins.

Vertical Temperature Fluctuations at Fixed Depths

Bell et al. [7] lowered 70 thermistors in a vertical chain at 1.4-m separation to a mean depth of 100 m and towed them at slow speed. From the measured data they constructed a one-dimensional (vertical) spectrum of internal wave amplitude. This is shown in Fig. 5b (their Fig. 1B). The abscissa

is $(\hat{n}_0/\hat{n})$ cpm, and the ordinate $(\hat{n}/\hat{n}_0)^2 \hat{F}_\zeta(\beta)$, in units of m²/cpm. It is important to note that the ordinate includes a (natural) integration over all horizontal wavenumbers and all frequencies which lie within the range of the length of the tow track and the duration of the experiment.

For purposes of making estimates we approximate the functional dependence of Bell et al. (Fig. 5b) by a simple power dependence,

$$y \approx x^a,$$

where

$$y = (\hat{n}/\hat{n}_0)\, \hat{F}_\zeta(\beta)$$

and

$$x = \frac{\hat{n}_0}{\hat{n}}\, \beta.$$

Thus,

$$y \approx \frac{3.184 \times 10^{-2}}{x^{2.2}}.$$

Now the integral over the entire spectrum from $x = 10$ to $x = 10^{-3}$ is

$$\int_{\Delta x} y dx = \int_{\Delta x} \frac{3.184 \times 10^{-2}}{x^{2.2}}\, dx = \frac{3.184 \times 10^{-2}}{-1.2}\, x^{-1.2}\Big|_{x_{\min}}^{x_{\max}}$$

$$= \frac{-3.184 \times 10^{-2}}{1.2} \left(\frac{1}{(10)^{1.2}} - \frac{1}{(10^{-3})^{1.2}} \right)$$

$$= 106.$$

However, the range of wavenumbers resolved by the experiment of Bell et al. was smaller. At the upper limit the array sampled the vertical temperature field at an effective spacing of 1.27 m between thermistors. The nominal limiting wavenumber was $1.27^{-1} = 0.787$, and the Nyquest limit was half of this, or 3.9×10^{-1} cpm (say 4×10^{-1} cpm). The lower limit in the vertical spectrum was obtained by using 16 decrements from the upper limit of size $4 \times 10^{-1}/16 = 2.5 \times 10^{-2}$ cpm, so that the lowest wavenumber resolved was 2.5×10^{-2} cpm, corresponding to a physical length of $2/(2.5 \times 10^{-2})$, or 80 m. The range of vertical wavenumbers was then

$$2.5 \times 10^{-2} < \beta < 4 \times 10^{-1} \text{ cpm}.$$

Now at a depth of 100 m the Vaisala frequency was measured at $\sim$ 5.0 cph. Hence $\hat{n}/\hat{n}_0 \approx 5/3 = 1.67$. Thus the range of parameter $x = (\hat{n}/\hat{n}_0)\beta$ was

$$4.2 \times 10^{-2} < x < 6.7 \times 10^{-1} \text{ cpm}.$$

The mean-square displacement in the range was then

$$\langle \zeta^2 \rangle = \int \left(\frac{\hat{n}}{n_0} \right)^2 \hat{F}_\zeta(\beta)\, d\left(\frac{\hat{n}}{\hat{n}_0}\, \beta \right) = \frac{-3.184 \times 10^{-2}}{1.2} \left[\frac{1}{(6.7 \times 10^{-1})^{1.2}} - \frac{1}{(4.2 \times 10^{-2})^{1.2}} \right]$$

$$= 1.148 \approx 1.2 \text{ m}^2.$$

Thus the mean-square vertical displacement over a vertical length of nominally 100 m centered at a depth of 100 m is $\sim$ 1.2 m². The mean-square *fluctuation* in temperature is then calculated from the measured value of the temperature gradient $d\theta/dy$ at that depth:

$$<\delta\theta^2(\Delta\beta,\ \hat{y})> = \left(\frac{d\theta}{dy}\right)^2 <\zeta^2>$$

$$= (0.025)^2 \times 1.2 = 7.5 \times 10^{-4}(\text{°C})^2.$$

This does not differ materially from the mean-square temperature fluctuations calculated from the horizontal spectra noted above. Using the same numerical values of k and n as before, we obtain

$$\sqrt{<\delta\phi_L^2>} = 1.40 \times 10^2 \times \sqrt{7.5 \times 10^{-4}} = 3.83 \text{ rad.}$$

Calculation of Temperature Fluctuations for Moored Spectra

Assume that a single point-source sensor is moored at a depth of 100 m, where it detects changes of temperature with time. A composite model of the spectrum of vertical displacement at this depth is given by GM72 [3]. We use this *moored spectrum* (MS) to calculate the mean-square fluctuation in temperature. Thus, the mean-squared vertical displacement is

$$<\zeta^2> = \int \hat{F}_\zeta(\omega)\, d\hat{\omega} = \frac{1}{\hat{n}} \frac{1}{2} \frac{1}{\pi^3} \frac{E\omega_i}{\hat{M}^2} \int \frac{(\omega^2 - \omega_i^2)^{1/2}}{\omega^3}\, d\hat{\omega}.$$

The definitions and values assigned to the symbols are taken from GM72 [3] and Bell et al. [7]:

$\hat{n}$ = Vaisala frequency—at 100 m depth, $\hat{n} = 5.0$ cph;
j_i = number of vertical modes—GM72 takes $j_i = 20$;
E = dimensionless energy—GM72 assigns $E = 2\pi \times 10^{-5}$;
ω_i = dimensionless inertial frequency—GM72 assigns

$$\omega_i = \frac{\hat{\omega}_i}{\hat{N}} = \frac{0.04\text{cph}}{3\text{cph}} = 1.333 \times 10^{-2};$$

$\hat{M}$ = spatial scale factor—GM72 assigns $\hat{M} = 1.22 \times 10^{-4}$; and
$\hat{N}$ = temporal scale factor—GH72 assigns $\hat{N} = 3$ cph.

With these assignments,

$$<\zeta^2> = \text{const} \times \int \frac{(\omega^2 - \omega_i^2)^{1/2}}{\omega^3}\, d\omega.$$

Now,

$$\frac{1}{\hat{n}\, 2\pi^3} \frac{E\omega_i \hat{N}}{\hat{M}^2} = \frac{1}{5.0} \times \frac{1}{2} \times \frac{1}{\pi^3} \times \frac{2\pi \times 10^{-5} \times 1.333 \times 10^{-2}}{(1.22 \times 10^{-4})^2} \times \frac{3.0}{1} = 0.5444\ \text{m}^2.$$

Next,

$$\int_{\Delta\omega} \frac{(\omega^2 - \omega_i^2)^{1/2}}{\omega^3}\, d\omega \rightarrow \int \frac{\sqrt{R}\, dx}{x^3},$$

where

$$R = a + bx + cx^2 \text{ and}$$
$$\Delta = 4ac - b^2.$$

In this case $a = \omega_i^2$, $b = 0$, $c = 1$, $\Delta = -4\omega_i^2$. Now from Gradshteyn and Ryzhik [9, p. 84],

$$\int \frac{\sqrt{R}\, dx}{x^3} = -\frac{\sqrt{R}}{2x^2} + \frac{1}{2} \int \frac{dx}{x\sqrt{R}} = -\frac{\sqrt{R}}{2x^2} + \frac{1}{2} \frac{1}{\sqrt{+\omega_i^2}} \arcsin \frac{2(-\omega_i^2)}{x\sqrt{-4(-\omega_i^2)}},$$

or

$$I_{\Delta\omega} = \int_{\Delta\omega} \frac{(\omega^2 - \omega_i^2)^{1/2}}{d\omega^3} = \left[-\frac{\sqrt{\omega^2 - \omega_i^2}}{2\omega^2} + \frac{1}{2\omega_i} \arcsin\left(-\frac{\omega_i}{\omega}\right) \right]_{\omega_{\min}}^{\omega_{\max}}$$

$$= -\frac{\sqrt{\omega_{\max}^2 - \omega_i^2}}{2\omega_{\max}^2} + \frac{1}{2\omega_i} \arcsin\left(-\frac{\omega_i}{\omega_{\max}}\right)$$

$$-\left[-\frac{\sqrt{\omega_{\min}^2 - \omega_i^2}}{2\omega_{\min}^2} + \frac{1}{2\omega_i} \arcsin\left(-\frac{\omega_i}{\omega_{\min}}\right) \right].$$

Assume that the entire GM72 spectrum is under consideration, i.e., $\hat{\omega}_{\max} = \hat{n}_0$, $\hat{\omega}_{\min} = \hat{\omega}_i$. Now,

$$\omega_{\max} = \frac{\hat{\omega}_{\max}}{\hat{n}_0} = 1$$

and

$$\omega_{\min} = \frac{\hat{\omega}_i}{\hat{n}_0} = \frac{0.04\,\text{cph}}{3\,\text{cph}} = 1.333 \times 10^{-2}.$$

Hence,

$$I_{\Delta\omega} = -\frac{\sqrt{1^2 - (1.333 \times 10^{-2})^2}}{2 \times 1^2} - \frac{1}{2 \times 1.333 \times 10^{-2}} \arcsin\left(-\frac{1.333 \times 10^{-2}}{1.0}\right)$$

$$-\left[-\frac{\sqrt{(1.333 \times 10^{-2})^2 - (1.333 \times 10^{-2})^2}}{2 \times (1.333 \times 10^{-2})^2} + \frac{1}{2 \times 1.333 \times 10^{-2}} \arcsin(-1) \right]$$

$$= -\frac{1}{2} + \frac{1}{2} - [-0 - 5.8919 \times 10^1] = 5.89 \times 10^1.$$

Thus, the mean-squared displacement for *all* frequencies is

$$\langle \zeta^2 \rangle = 0.5444 \times 5.89 \times 10^1 = 3.21 \times 10\,\text{m}^2$$

and

$$\sqrt{\langle \zeta^2 \rangle} = 5.7\ \text{m}.$$

If the observation time is restricted to be less than ω_i^{-1} (= 25 h/cycle), then the lower limit of integration is increased. Take, for example, a time of 1 h. Then $\hat{\omega}_{\min} = 1$ cph, and

$$\omega_{\min} = \frac{\hat{\omega}_{\min}}{\hat{n}_0} = \frac{1\ \text{cph}}{3\ \text{cph}} = 3.33 \times 10^{-1}.$$

Hence,

$$I_{\Delta\omega} = \frac{-1}{2 \times 3.33 \times 10^{-1}} \arcsin(-1) = 2.36,$$

so that

$$\langle \zeta^2 \rangle = 0.544 \times 2.36 = 1.28\ \text{m}^2.$$

Finally, if the observation time is 10 min, we take $\omega_{\min} \approx 6$ cph, so that

$$\omega_{\min} = \frac{6}{3} = 2,$$

$$I_{\Delta\omega} = \frac{-1}{2 \times 2} \arcsin(-1) = 0.39,$$

and

$$<\zeta^2> = 0.544 \times 0.39 = 0.21 \text{ m}^2.$$

The mean-square temperature fluctuation of a moored sensor at a depth of 100 m in the three cases is then calculated by use of the Bell et al. temperature gradient of 0.025°C [7]:

For $\omega_{min} = \omega_i$

$$<\delta\theta^2> = 32.1 \times (0.025)^2 = 0.02 \ (^\circ\text{C})^2$$

and

$$\sqrt{<\delta\theta^2>} = 0.14 \ ^\circ\text{C}.$$

For $\omega_{min} = 25\omega_i$

$$<\delta\theta^2> = 1.28 \times (0.025)^2 = 8.0 \times 10^{-4} \ (^\circ\text{C})^2$$

and

$$\sqrt{<\delta\theta^2>} = 2.8 \times 10^{-2} \ ^\circ\text{C}.$$

For $\omega_{min} = 150\omega_i$

$$<\delta\theta^2> = 0.21 \times (0.025)^2 = 1.3 \times 10^{-4} \ (^\circ\text{C})^2$$

and

$$\sqrt{<\delta\theta^2>} = 1.14 \times 10^{-2} \ ^\circ\text{C}.$$

To find the corresponding rms phase fluctuation we must be given the correlation time T_c, the integration time T, and the phase conversion factor $C_{\theta T}$. In the absence of data, we assume

$$2TT_c = O(1) \ \text{s}^2$$

and

$$|C_{\theta T}| = |C_{\theta L}| = 1.40 \times 10^2.$$

Then the three cases become:

$\omega_{min} = \omega_i = 0.04$ cph, $\sqrt{<\delta\theta^2>} = 1.4 \times 10^2 \times 0.14 = 19.6$ rad;

$\omega_{min} = 25\omega_i = 1$ cph, $\sqrt{<\delta\theta^2>} = 1.4 \times 10^2 \times 2.8 \times 10^{-2} = 3.92$ rad;

and

$\omega_{min} = 150\omega_i = 6$ cph, $\sqrt{<\delta\theta^2>} = 1.4 \times 10^2 \times 1.14 \times 10^{-2} = 1.60$ rad.

Thus, if we allow the fiber to report all temperature fluctuations for 25 h (1 cycle at $\omega_i = 0.04$ cph), the rms phase fluctuation is very large (19.6 rad). If, on the other hand, the cutoff is 6 cycle/h and $\theta \approx 10$ min observation, then the rms phase becomes 1.6 rad.

With these results the calculation of mean-square vertical displacement of internal waves from towed spectra (in coordinates α_1 and α_2) and moored spectra (in coordinate ω) has been completed for particular selections of depth, range, and size of the fiber-optic sensor. Corresponding to these space-time scales, we have calculated mean-square temperature fluctuations. An additional calculation can be made when the fiber has finite mass, and hence when there is a lag before steady state is reached. Let $h(t)$ represent the difference in temperature between the surface of the fiber and the center; then

$$h(t) = \delta(t-0) - \frac{1}{T} e^{-t/T}, \quad 0 \leqslant t < T \quad \text{(units: s}^{-1}\text{)}$$

$$= 0 \quad \text{outside the interval } 0,\ T,$$

in which T is the time constant of the equivalent filter. The transfer function of this filter is

$$H(\omega) = \frac{i\omega T}{1 + i\omega T},$$

whose squared modulus is

$$|H(\omega)|^2 = \frac{(\omega T)^2}{H(\omega T)^2}.$$

Thus the required integral is

$$\int_{\omega_{min}}^{\omega_{max}} \frac{(\omega^2 - \omega_i^2)^{1/2}}{\omega^3} \times \frac{(\omega T)^2}{[1 + (\omega T)^2]}\, d\omega \propto \int \frac{\sqrt{R}\ dx}{X[1 + \beta X^2]}.$$

This integral can be evaluated by numerical integration. However, for values of T such that $\omega^2 T^2 >> 1$ the calculations made above are seen to be valid. Figure 6, a plot of $|H(\omega)|^2$, shows the effective window.

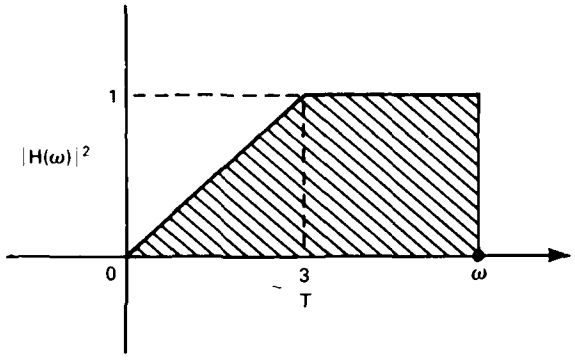

Fig. 6 — $H(\omega)^2$ vs ω

We next turn to vertical displacements (hence temperature fluctuations) of much smaller space-time scales, namely the microtemperature field of the ocean.

Microtemperature Structure of the Ocean

The microtemperature structure of the ocean has been measured and analyzed at an increasing pace in the last 15 years, and a wealth of data is now readily accessible. We select from the many articles and reports a few examples which are chosen for their immediate usefulness in making numerical estimates of the effects of microstructure on the phase stability of laser light in a fiber-optic hydrophone.

We begin with Gregg and Cox [10]. They measured vertical gradients of temperature in the ocean on a millimeter scale in the depth range from 100 m to 500 m. The site of measurement was the San Diego Trough. The method used consisted of a free-fall probe with no connections to the surface. Recovery of the measurement package allowed data processing of the tape-recorded temperature records; these records were continuous. The analysis, however, was based on a sampling procedure in which one data point was taken every 1.5 mm. The mean temperature gradient over the entire 100- to 500-m record was $+9.4 \times 10^{-5}$°C/cm (a positive gradient means temperature increasing upwards).

Chosen for analysis were two sections of record ~7 m long at 302-m and 320-m depth. They are reproduced here as Figs. 7 and 8 from Figs. 8 and 9 of Ref. 10.

We discuss Fig. 7 first and note:

- The mean vertical temperature gradient over the record was -3.4×10^{-5} °C/cm.
- The rms gradient (signs omitted) was 2.4×10^{-4} °C/cm.
- A net inversion of temperature of magnitude ~ 2×10^{-2} °C occurred over a vertical thickness of 0.5 m of medium.
- Although $d\theta/dz$ exhibited random structure, $\theta(z)$ was relatively smooth.

Figure 8 exhibits the same behavior at 320 m depth:

- The mean gradient was -2.2×10^{-5} °C/cm.
- The rms gradient was 7.2×10^{-4} °C/cm.
- An inversion of 2.7×10^{-2} °C occurred in about 2 m of vertical thickness.

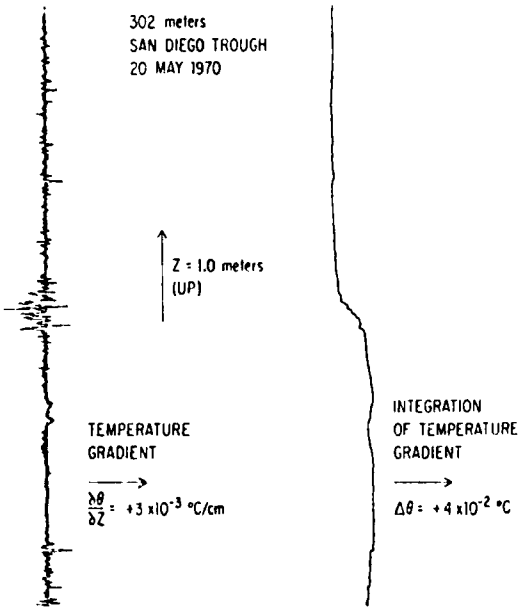

Fig. 7 — Vertical component of temperature gradient and its integral at 302 m [10, Fig. 8]

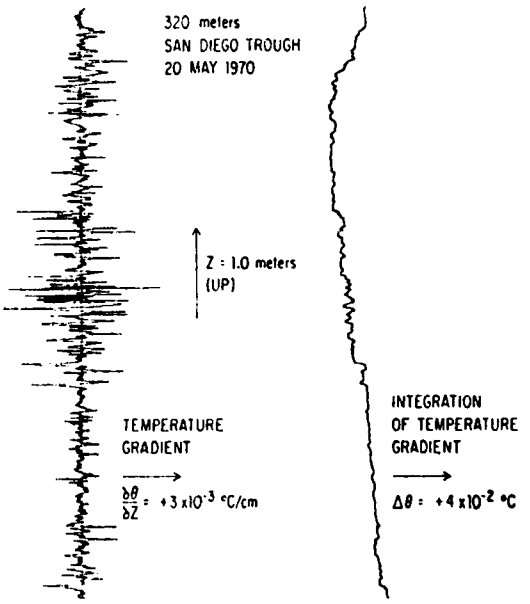

Fig. 8 — Vertical component of temperature gradient and its integral at 320 m [10, Fig. 9]

Stommel and Fedorov [11] made continuous vertical temperature records from 0 to 500-m depth in the Phillipine Sea off Mindanao and off Timor over a 10-mile-square range. Figures 9a and 9b (Figs. 3 and 4 of Ref. 11) show the salinity, temperature, and depth traces of Station 13 off Timor and Station 21 off Mindanao. Examination of these traces led them to believe that sharp vertical gradients of temperature about 2 to 40 m in thickness existed in *lamina* (or stratification) which extended *horizontally*

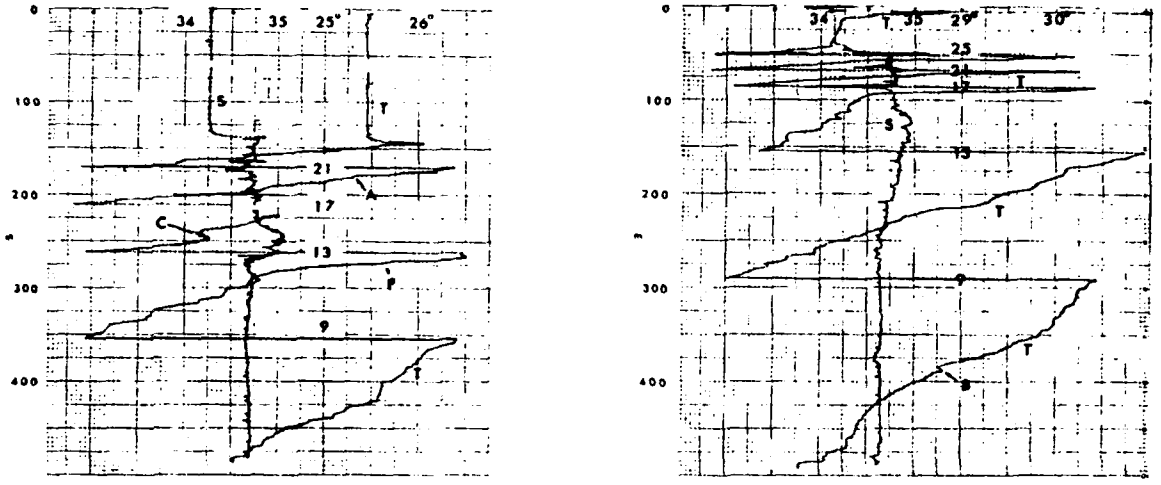

Fig. 9 — Photographic copy of actual STD trace of STD station 13 off Timor [11, Fig. 3] (a) and STD station 21 off Mindanao [11, Fig. 4] (b). The depth scale is 500 meters, each small division being 5 meters. The salinity curve is labeled *S*, the scale of salinity is labeled at two points 34 and 35, thus each smallest division in the abscissa is 0.05‰. The temperature curve is labeled *T* (the labels *A*, *C*, and *P* refer to particular points of interest on the temperature curve. At the top two temperature points on the abscissa are labeled 25° and 26°C, thus each smallest division is 0.05°C. The temperature curve has origin reset at successive depths where it tends to go off scale. This is done in steps of 4°C as indicated by the numerals 21, 17, 13, 9, thus point *A* is at 21.32°C. The pens cannot both transverse the same path mechanically so the *temperature curve* is offset downward by 5 meters and hence always reads 5 meters too deep. On tracings this has been allowed for and corrected. On this photograph of the original it must remain uncorrected. The salinity scale is not offset in depth. A uniform correction has been determined for the STD records, and is described in paragraph 2 of the text, but has not been applied to any of the data as it is only a small constant value. All temperatures should be corrected by 0.07°C, all salinities by −0.09‰.

from 2 to 20 km. Vertical scales of less than 2 m were not clearly resolved by the salinity, temperature, and depth measurements (STD) actually obtained. However, the trace pen was held stationary for 1-min intervals, and the heaving of the ship effectively caused the tethered sensor to sample the vertical temperature structure with greater resolution. Figure 10 of their article shows this sampling at a 275-m depth (point P of our Fig. 9a, their Fig. 3). From this figure it is deduced that:

- The lowest mean temperature was 17.26°C at minute 9 of the record.
- The highest mean temperature was 17.97°C at minute 39 .
- The total range of vertical displacement of the isotherm due to internal waves was 5 meters.
- The homogeneous lamina at P was perhaps 3 m thick.
- The mean temperature gradient at station 13 between 200 and 300 m was 4×10^{-2} °C/m.
- Inside the lamina P the gradient was less than 3×10^{-3} °C/m.
- Directly above and below the lamina the temperature gradient was > 0.35°C/m (3.5×10^{-3} °C/cm).
- The horizontal scale of the lamina exceeded 2 km.

Stommel and Fedorov note that other authors (for instance, Liebermann [12]) have measured much smaller horizontal scales. They conjecture that the observed lamina of their own measurements may be corrugated so that a horizontally moving probe would move in and out of the layer, thus accounting for smaller scales. Liebermann [12] measured temperature fluctuations in the ocean along a *horizontal* line by means of a probe mounted on a submarine. His work is reviewed briefly in Appendix G. Here we write again his main analytical result, that the mean value of the fluctuation in temperature gradient is given by the formula

$$<[\Delta T(d)]^2> = 2<T^2>\left[1 - \frac{30}{29}\, e^{-\frac{d}{60}} + \frac{1}{29}\, e^{-\frac{d}{2}}\right] \quad \text{(units: (°C)}^2\text{)},$$

in which the unit of range d is cm, and $<T^2>$ is the spatial variance of the fluctuating temperature. The horizontal correlation length $l_{c\theta}$ was estimated by Liebermann to be 60 cm.

It is somewhat difficult to gather from this work what the value of $<T^2>$ should be. On p. 565 (of Ref. 12) there appears the sentence, "The average temperature deviation of this record is 0.04°C...." The record in question was some 30 m long, taken at a depth of $\sim$50 m in the continental waters off the U.S. Actually, a variance could be obtained from the record by subtracting out the mean, selecting a number of data points, squaring the temperature fluctuation at these data points, and adding all the squares. The sum would be the variance. The square root of the sum would be the standard deviation. This has not been done. Since we desire to make Liebermann's data compatible with GM72 [3], we will proceed in the next section on the basis of this latter interpretation.

The Tow Spectrum of Liebermann as Interpreted by GM72 [3]

Liebermann [12] measured an autocorrelation of temperature fluctuation of form $\sim e^{-\rho/60}$, in which ρ is the log distance in cm and 60 cm is the correlation distance. For convenience we write this as

$$R(\rho) \propto \exp(-l_{c\theta}^{-1}\,\rho).$$

The power spectrum of these temperature fluctuations can be obtained by use of the Wiener-Kinchine theorem:

$$F_R(\alpha) \propto 4\int_0^\infty \exp(-l_{c\theta}\rho)\cos\alpha\rho\frac{d\rho}{2\pi}$$

$$\propto \frac{2l_{c\theta}^{-1}}{\pi}\frac{1}{(l_{c\theta}^{-2}+\alpha^2)}$$

(for derivation see p. 312 of [9]). Here α takes on positive values only. The constant of proportionality is the mean-square fluctuation (or variance) of the random temperature field for all spatial and temporal microstructure scales. Thus the α-spectrum, or towed spectrum (TS), of Liebermann as interpreted by GM72 [3] has the form

$$F_T = <\delta\theta^2>\frac{2}{\pi}\left(\frac{l_{c\theta}^{-1}}{l_{c\theta}^{-2}+\alpha^2}\right).$$

Now at fixed depth y the temperature power spectrum is related to the vertical-displacement power spectrum F_ζ:

$$F_T = \left(\frac{d\theta}{dy}\right)^2 F_\zeta$$

(see p. 237 of GM72 [3]). Actually, to obtain a universal representation, GM72 plots $\hat{n}\hat{F}_\zeta(\alpha_1)$ vs α_1, in which the following definitions hold:

$\hat{n}$ = dimensional Vaisala frequency (units: cycle/h),

$\hat{F}_\zeta(\alpha_1)$ = dimensional power spectrum for vertical displacement (units: m^3/cycle), and

α_1 = horizontal component of wavenumber (units: cycle/m).

To check this representation by GM72 of Liebermann's work, we choose a depth of 30 m, such that $d\theta/dy = 0.2$ °C/m. The towed spectrum of Liebermann's data extends roughly from 0.1 to 10 cycle/m. GM72 interprets Liebermann's measured correlation length ($l_{c\theta} = 60$ cm) as $\alpha_0^{-1} = O(1\text{ m})$. Inside the selected wavenumber band, let us choose $\alpha_1 = 1$ cpm as a check point, and let us take $\hat{n} = 6$ cycle/m at the selected depth. Thus, for $<\delta\theta^2> = (0.02)^2$,

$$\hat{n}\,\hat{F}_\zeta(\alpha_1) = \frac{(0.02)^2}{(0.2)^2}\frac{2}{\pi}\left(\frac{1}{1^2+1^2}\right)\times 6$$

$$= \frac{6}{\pi}\times 10^{-2} \approx 2\times 10^{-2}\ m^3h^{-1}.$$

This checks with the value shown in Fig. 2 (Fig. 4 of GM72). If we were to construct a power spectrum of microtemperature fluctuations using Liebermann's work, we could use this result to find one point on the spectrum:

$$F_T = (0.2)^2\times\frac{6}{\pi}\times 10^{-2}\times\frac{1}{6} = \frac{4}{\pi}\times 10^{-4}\quad\left[\text{units: }\frac{(°C)^2}{\text{cpm}}\right].$$

These formulas will be used in the next section.

Calculation of Effect of Temperature Microstructure on the Phase of a Fiber-Optic Hydrophone

As noted earlier, this report uses Liebermann's data [12] as interpreted by GM72 [3] to find the effect of temperature microstructure on the phase stability of a fiber-optic hydrophone. From the previous section,

$$F_T(\alpha) = <\delta\theta^2> \frac{2}{\pi}\left[\frac{l_{c\theta}^{-1}}{l_{c\theta}^{-2} + \alpha^2}\right] \quad \text{(units: } (\text{°C})^2 \cdot \text{m)}.$$

We want to find the band-limited variance of temperature fluctuations:

$$<\delta\theta^2(\Delta\alpha)> = \int_{\Delta\alpha} <\delta\theta^2> \frac{2}{\pi}\left[\frac{l_{c\theta}^{-1}}{l_{c\theta}^{-2} + \alpha^2}\right] d\alpha \quad \text{(units: } (\text{°C})^2).$$

The integral is elementary:

$$<\delta\theta^2(\Delta\alpha)> = <\delta\theta^2> \frac{2}{\pi}\left[\arctan(\alpha_{\max} l_{c\theta}) - \arctan(\alpha_{\min} l_{c\theta})\right].$$

Now choose a fiber L units long and assume that the fiber spatially detects the temperature fluctuations along its entire length. Then the bandwidth of wavenumbers extends from ∞ to $1/L$. Thus,

$$<\delta\theta^2(\Delta\alpha)> = <\delta\theta^2> \frac{2}{\pi}\left[\arctan\infty - \arctan\frac{l_{c\theta}}{L}\right].$$

For example, let $L = 40$ cm and $l_{c\theta} = 60$ cm; then

$$<\delta\theta^2(\Delta\alpha)> = (0.02)^2 \frac{2}{\pi}\left[\frac{\pi}{2} - \arctan\frac{60}{40}\right]$$

$$= 1.50 \times 10^{-4} \quad \text{(units: } (\text{°C})^2).$$

Similarly, for $L = 1$ cm,

$$<\delta\theta^2(\Delta\alpha)> = 4.24 \times 10^{-6} \quad \text{(units: } (\text{°C})^2).$$

The effect of these temperature fluctuations on the microstructure scale is found from the formula previously derived (in the section "Calculation of the Mean-Square Fluctuation in Temperature over a Towed Fiber"):

$$\sqrt{<\delta\phi^2>} = 1.400 \times 10^2 \sqrt{<\delta\theta^2(\Delta\alpha)>}.$$

Thus, the mean-square phase fluctuation caused by temperature microstructure is calculated to be

$$\sqrt{<\delta\phi^2>} = 1.400 \times 10^2 \times \sqrt{1.5 \times 10^{-4}} = 1.7 \text{ rad, for } L = 40 \text{ cm,}$$

and

$$\sqrt{<\delta\phi^2>} = 1.400 \times 10^2 \times \sqrt{4.24 \times 10^{-6}} = 0.29 \text{ rad, for } L = 1 \text{ cm.}$$

The magnitudes of these phase disturbances are contingent on the selection by GM72 [3] of $\delta T = 0.02$ °C and $\delta T/\delta\hat{y} = 0.2$°C/m. A nearly similar result is obtained if we use Liebermann's measurements directly [12]. As explained in Appendix G, Liebermann measured an average fluctuation of about 0.04°C over a correlation distance of about 60 cm. By extrapolation the rms average fluctuation over a distance of 1 cm is about 3.4×10^{-3}°C, and over a distance of 40 cm it is 3.9×10^{-2}°C. Given the uncertainties of the precision of measurement, these values are near enough to make the interpretation of Liebermann's work by GM72 a reasonable model.

CONCLUSIONS

The temperature field in the ocean is subject to spatial and temporal fluctuations of two distinctly different scales. The larger scales, of the order of hundreds of meters in space and fractions to several hours in time, are caused by internal waves. The smaller scales (microscales), of the order of millimeters in space and seconds in time, are caused by velocity turbulence and thermal diffusion. We have

calculated the effect of both these types of temperature fluctuations on the phase stability of an optical-fiber hydrophone when the summation is nearly incoherent. The results of the analysis appear in the form of space (subscript L) and time (subscript T) phase fluctuations:

$$(\delta\phi_L)_{\text{rms}} = C_{\theta L}\sqrt{2LL_c}\,\delta\theta_{\text{rms}}(L),$$

and

$$(\delta\phi_T)_{\text{rms}} = C_{\theta T}\sqrt{2TT_c}\,\delta\theta_{rms}(T),$$

in which $(\delta\theta_L)_{\text{rms}} = \sqrt{<\delta\theta^2(\Delta\alpha)>}$ and $(\delta\theta_T)_{\text{rms}} = \sqrt{<\delta\theta^2(\Delta\omega)>}$, where $<\delta\theta^2>$ is the mean-squared fluctuation of temperature over either a band $\Delta\alpha$ of wavenumbers or a band $\Delta\omega$ of frequencies. To obtain the latter we have used the work of Garrett and Munk and of Liebermann. Table 3 shows $\delta\theta_{\text{rms}}$ calculated for specific choices of spectrum, fiber length, and depth of ocean, based upon the assumption that $|2LL_c| = O(1)$ m^2 and $|2TT_c| = O(1)$ s^2.

Table 3—Calculated RMS Temperature Fluctuations in the Ocean and Corresponding RMS Phase Fluctuations

Method of Analysis	Literature Source of Spectrum or Correlation	Length of Fiber (m)	Depth of Center of Fiber in Ocean (m)	RMS Vertical Displacement of Ocean in Spectral Window (m)	RMS Temperature Fluctuation in Spectral Window (°C)	RMS Phase Fluctuation for $\|2LL_c\| = O(1)$m^2 or $\|2TT_c\| = O(1)$s^2 (rad)
Power spectrum of internal waves						
Horizontal	GM72 [3] (Towed)	1000	100	1.15	0.029	4.04
Vertical	GM72 [3] (Dropped)	100	100	1.1	0.027	3.83
Temporal	GM72 [3] (Moored)	100	100	5.7* 1.13† 0.46‡	0.14* 0.028† 0.0114‡	19.6* 3.92† 1.6‡
Spatial correlation of temperature microstructure	Liebermann [12] (Correlation length = 60 cm)	0.4 0.01	30 to 60 30 to 60	– –	0.012 0.0021	1.7 0.29

*$\omega_{\min}/\omega_i = 1$

†$\omega_{\min}/\omega_i = 25$ $\quad \Delta\omega$ band = $\begin{cases}\omega_{\max} = 3 \text{ cph} \\ \omega_{\min} = 0.049 \text{ cph}\end{cases}$

‡$\omega_{\min}/\omega_i = 150$

The significant temporal contribution to the power spectrum of internal waves is contained in the band between the inertial frequency (0.04 cph in our latitude) and the Vaisala frequency (3 cph and upward depending on depth). The frequencies of interest for a fiber-optic hydrophone are currently above 10 Hz; therefore, it is concluded that the temperature fluctuations in time associated with internal waves will not directly contribute to fiber-optic hydrophone noise. Additional noise will not be present even if a fiber-optic sensor is towed at normal speeds through the temperature of internal waves on a level track.

Lack of data has prevented the determination of temporal dependence of temperature microstructure; however, spatial calculations indicate that a reduction of unwanted phase shifts due to temperature microstructure can be achieved by the use of an extended sensor (see Table 3, "Spatial correlation of temperature microstructure"). When additional data concerning the relative temperature-induced phase

shifts of piezoelectric and fiber-optic sensors are available, analysis of the temporal nature of temperature microstructure may be valuable.

The rms phase fluctuations due to temperature effects of both internal wave and microstructure indicate that homodyne fading could be significant as the operating point is shifted away from the optimum phase setting. The magnitude of these fluctuations will be important if homodyne detection with feedback for optical alignment is used. The frequency response of a feedback system would depend on the temporal dependence of internal waves and microstructure.

It is important to note that the results listed in Table 3 are strongly depth dependent and that they are narrowly contingent on the use of *band-limited* spectra. Furthermore, we have assumed that the temperature fluctuations are instantly sensed by the optical fiber, and we have thereby neglected the finite time effects of thermal conduction. Formulas which include conduction have been, however, explicitly derived in this report. It is natural to expect that thermally insulated fibers will exhibit greatly reduced sensitivity to ocean temperature fluctuations.

In a separate analysis we have derived formulas for the S/N ratio of fiber-optic hydrophones in which the noise N includes laser jitter, environmental noise, and the customary shot noise.

ACKNOWLEDGMENTS

The author wishes to thank Dr. D. Palmer, Dr. J. Bucaro, and Mr. J. Cole of the Acoustics Division for illuminating discussions on the material covered in this report. Mr. Cole also contributed to the "Conclusions" section.

REFERENCES

1. G.I. Taylor, "Diffusion by Continuous Movements," Proc. London Math. Soc. **20**, 196 (1922).

2. V.I. Tatarskii, "The Effects of the Turbulent Atmosphere on Wave Propagation," Israel Program for Scientific Translations, Jerusalem, 1971, p. 181. (Available from the U.S. Department of Commerce, National Technical Information Service, Springfield, VA 22151.)

3. C. Garrett and W. Munk, "Space-Time Scales of Internal Waves," Geophys. Fluid Dyn. **3**, 225 (1972).

4. M. Born and E. Wolf, *Principles of Optics*, 5th ed., Pergamon Press, New York, 1975, Sect. 10.3, p. 499.

5. H. Melchior, "Sensitive High Speed Photodetectors for the Demodulation of Visible and Near Infrared Light," J. Luminescence **7**, 390 (1973).

6. C. Garrett and W. Munk, "Space-Time Scales of Internal Waves: A Progress Report," J. Geophys. Res. **80**, 291 (1975).

7. T.H. Bell, Jr., et al. "Internal Waves: Measurements of the Two-Dimensional Spectrum in Vertical-Horizontal Wave Number Space," Science **189**, 632 (1975).

8. W. H. Munk, "Sound Channel in an Exponentially Stratified Ocean, with Application to SOFAR," J. Acoust. Soc. Am. **55**, 220 (1974).

9. I.S. Gradshteyn and I.M. Ryzhik, *Tables of Integrals, Series and Products*, 4th ed., Academic Press, New York, 1965.

10. M.C. Gregg and C.S. Cox, "Measurements of the Oceanic Microstructure of Temperature and Electrical Conductivity," Deep-Sea Res. **18**, 925 (1971).

11. H. Stommel and K.N. Fedorov, "Small Scale Structure in Temperature and Salinity near Timor and Mindanao," Tellus **19**, 306 (1967).

12. L. Liebermann, "The Effect of Temperature Inhomogeneities in the Ocean on the Propagation of Sound," J. Acoust. Soc. Am. **23**, 563 (1951).

Appendix A

CORRELATION FACTORS

From the "Procedure of Analysis" section we can find that

$$<\delta\phi_L^2> = 2C^2 L \int_0^L \left(1 - \frac{\xi}{L}\right) R_{\delta\theta}(\xi)\, d\xi,$$

where the units of C are rad/°C · m, of L are m, of $R_{\delta\theta}$ are $(°C)^2$, and of ξ are m.

Now assume that $R_{\delta\theta}(\xi)$ is Gaussian,

$$R_{\delta\theta} = <\delta\theta^2> e^{-\xi^2/2L_c^2},$$

then

$$<\delta\phi_L^2> = 2C^2 L <\delta\theta^2> \left[\int_0^L e^{-\xi^2/2L_c^2} d\xi - \int_0^L \frac{\xi}{L} e^{-\xi^2/2L_c^2} d\xi\right].$$

Now [A1]

$$\int_0^L e^{-\xi^2/2L_c^2} d\xi = \frac{\sqrt{\pi}}{2\left(\frac{1}{\sqrt{2}L_c}\right)} \Phi\left(\frac{L}{\sqrt{2}L_c}\right),$$

$$\Phi(x) = \frac{2}{\sqrt{\pi}} \int_0^x e^{-t^2} dt,$$

and

$$\frac{1}{L}\int_0^L \xi\, e^{-\xi^2/2L_c^2} d\xi = \frac{L_c^2}{L}\left(1 - e^{-L^2/2L_c^2}\right).$$

Thus,

$$<\delta\phi_L^2> = 2C^2 L <\delta\theta^2> \left[L_c\sqrt{\frac{\pi}{2}}\, \Phi\left(\frac{L}{\sqrt{2}L_c}\right) - \frac{L_c^2}{L}\left(1 - e^{-L^2/2L_c^2}\right)\right].$$

When $L_c << L$, the correlation factor is $L_c\sqrt{\frac{\pi}{2}}\, \Phi(\infty) \rightarrow L_c\sqrt{\frac{\pi}{2}}$.

The function $1 - \frac{\xi}{L}$ acts as a "window" to the correlation function. Assume that $R_{\delta\theta}(\xi)$ is periodic, say $<\delta\theta^2> \cos\alpha L$. Then

$$K = \int_0^L \left(1 - \frac{\xi}{L}\right) \cos\alpha\xi\, d\xi = \frac{L}{2}\left(\frac{\sin\alpha L/2}{\alpha L/2}\right)^2.$$

If $\frac{kL}{2} \ll 1$, then the correlation length is very large and the correlation factor K is $L/2$. If $kL/2 \gg 1$, then there are numerous oscillations, the correlation length is very small, and the correlation factor $K \to 0$.

REFERENCE

A1. I.S. Gradshteyn and I.M. Ryzhik, *Tables of Integrals, Series and Products*, 4th ed., Academic Press, New York, 1965, p. 306.

Appendix B

MEASURED VS THEORETICAL AUTOCORRELATIONS

A review of an analysis by Corcos [B1] is presented here.

Let $N(\mathbf{x}, t)$ be the instantaneous disturbance of the medium at point $\mathbf{X}$, and let $<N(\mathbf{x})>$ be its average value over a long duration. The fluctuation of N is defined as $n(\mathbf{x}, t) = N(\mathbf{x}, t) - <N(\mathbf{x})>$. It is considered a random variable in space and time and possesses an autocorrelation function

$$R(\boldsymbol{\zeta}, \tau) = <n(\mathbf{x}, t)\, n(\mathbf{x} + \boldsymbol{\zeta}, t + \tau)>$$

and a power spectrum (or energy density)

$$F(\boldsymbol{\alpha}, \omega) = \int\int\int\int_{-\infty}^{\infty} R(\boldsymbol{\zeta}, \tau)\, \exp[+ i(\omega\tau - \boldsymbol{\alpha} \cdot \boldsymbol{\zeta})]\, \frac{d\tau\, d\boldsymbol{\zeta}}{(2\pi)^4}.$$

The partial Fourier transform, or cross-spectral density, is defined as,

$$F(\boldsymbol{\zeta}, \omega) = \int_{-\infty}^{\infty} R(\boldsymbol{\zeta}, \tau)\, e^{+i\omega\tau} \frac{d\tau}{2\pi}.$$

Now consider the measurement instrument to be a filter with weighting function (or window) $h(\mathbf{s}, \eta)$ (units: $m^{-3}s^{-1}$). The *measured disturbance* is then the convolution,

$$n(\mathbf{x}, t) = \int\int\int\int_{-\infty}^{\infty} n(\mathbf{x}, t)\, h(\mathbf{s} - \mathbf{x}, \eta - t)\, ds^3\, d\eta.$$

The measured autocorrelation over volume V and time T is

$$R_m = \int\int \cdots \int h(\mathbf{s}-\mathbf{x}, \eta-t)\, n(\mathbf{x}, t)\, n(\mathbf{x}+\boldsymbol{\zeta}, t+\tau)\, h[\mathbf{q} - (\mathbf{x} + \boldsymbol{\zeta}), \xi - (t + \tau)]$$
$$d^3\mathbf{s}\, d^3\mathbf{q}\, d\xi\, d\eta \frac{d^3\mathbf{x}\, dt}{VT}.$$

Let $\mathbf{s} - \mathbf{x} = \mathbf{a}$, $\mathbf{q} - (\mathbf{x} + \boldsymbol{\zeta}) = \mathbf{b}$, $\eta - t = c$, and $\xi - (t + \tau) = d$, and consider spatial coordinates first. Then for stationary homogeneous statistics of n the integrand has the form

$$h(\mathbf{a})\, n(\mathbf{s} - \mathbf{a})\, n(\mathbf{q} - \mathbf{b})\, h(\mathbf{b}).$$

The total spatial lag is

$$\mathbf{s} - \mathbf{a} - \mathbf{q} + \mathbf{b} = \mathbf{s} - \mathbf{q} + \mathbf{b} - \mathbf{a} = \boldsymbol{\zeta} + \mathbf{b} - \mathbf{a}.$$

Hence an integration over $d^3\mathbf{x}$ yields the autocorrelation in space

$$R(\boldsymbol{\zeta} + \mathbf{b} - \mathbf{a}).$$

A similar consideration holds for the temporal coordinate so that an integration over dt yields

$$R(\tau + d - c).$$

Thus the measured autocorrelation function is

$$R_m(\boldsymbol{\zeta}, \tau) = \int\int_{-\infty}^{\infty} \cdots \int h(\mathbf{a}, c)\, R(\boldsymbol{\zeta} + \mathbf{b} - \mathbf{a}, \tau + d - c)\, h(\mathbf{b}, d)\, d^3\mathbf{a}\, d^3\mathbf{b}\, dc\, dd.$$

This form allows us to derive the measured cross-spectral density at zero lag ($\zeta = 0$), which is the ordinary frequency spectrum $\Phi_m(\omega)$:

$$\Phi_m(\omega) = F_m(0, \omega) = \int_{-\infty}^{\infty} R_m(0, \tau)\, e^{i\omega\tau} \frac{d\tau}{2\pi}$$

$$= \int_{-\infty}^{\infty} e^{i\omega\tau} \frac{d\tau}{2\pi} \int\int_{-\infty}^{\infty} \cdots \int h(\mathbf{a}, c) R(\mathbf{b} - \mathbf{a}, \tau + d - c)\, h(\mathbf{b}, d)\, d^3\mathbf{a}\, d^3\mathbf{b}\, dc\, dd.$$

An oft-encountered case is the one in which the transducer instantaneously senses the effect of the environmental disturbance. In this case

$$h(\mathbf{a}, c)\, h(\mathbf{b}, d) = h(\mathbf{a})\, h(\mathbf{b})\, \delta(c - d).$$

When this applies, the following formulas hold:

$$\Phi_m(\omega) = \int_{-\infty}^{\infty} e^{i\omega\tau} \frac{d\tau}{2\pi} \int\int_{-\infty}^{\infty} \cdots \int h(\mathbf{a}) R(\mathbf{b} - \mathbf{a}, \tau) h(\mathbf{b}) d^3\mathbf{a} d^3\mathbf{b}$$

$$= \int\int_{-\infty}^{\infty} \cdots \int h(\mathbf{a}) F(\mathbf{b} - \mathbf{a}, \omega)\, h(\mathbf{b})\, d^3\mathbf{a}\, d^3\mathbf{b}.$$

Now let

$$\mathbf{b} - \mathbf{a} = \mathbf{e},$$

then

$$\Phi_m(\omega) = \int\int_{-\infty}^{\infty} \cdots \int F(\mathbf{e}, \omega)\, h(\mathbf{a})\, h(\mathbf{a} + \mathbf{e})\, d^3\mathbf{a}\, d^3\mathbf{e}.$$

From this one can identify a transducer response function $H(\mathbf{e})$,

$$H(\mathbf{e}) = \int_{-\infty}^{\infty} h(\mathbf{a})\, h(\mathbf{a} + \mathbf{e})\, d^3\mathbf{a}.$$

This is sometimes called the autocorrelation function of the filter window. The measured frequency spectral density is then

$$\Phi_m(\omega) = \int\int_{-\infty}^{\infty} \cdots \int F(\mathbf{e}, \omega)\, H(\mathbf{e})\, d^3\mathbf{e}.$$

Now $F(\mathbf{e}, \omega)$ is related to the power spectrum of the total (temporal-spatial) disturbance, $|M(\boldsymbol{\alpha}, \omega)|^2$:

$$F(\mathbf{e}, \omega) = \int_{-\infty}^{\infty} |M(\boldsymbol{\alpha}, \omega)|^2\, e^{-\boldsymbol{\alpha} \cdot \mathbf{e}}\, d^3\boldsymbol{\alpha},$$

where

$$|M(\boldsymbol{\alpha}, \omega)|^2 = \int\int_{-\infty}^{\infty} \int\int R(\boldsymbol{\zeta}, \tau)\, e^{-i(\omega\tau + \boldsymbol{\alpha} \cdot \boldsymbol{\zeta})} \frac{d\tau\, d^3\boldsymbol{\zeta}}{(2\pi)^4}.$$

A more general transducer response function occurs when the temporal response is finite in time. Let

$$d - c = g,$$

so that

$$H(\mathbf{e}, g) = \int\int_{-\infty}^{\infty} \cdots \int h(\mathbf{a}, c)\, h(\mathbf{a} + \mathbf{e}, c + g)\, d^3\mathbf{a}\, dc.$$

The measured temporal spectral density is then

$$\Phi_m(\omega) = \int\int_{-\infty}^{\infty} \cdots \int F(\mathbf{e}, g, \omega)\, h(\mathbf{e}, g) d^3\mathbf{e} dg,$$

where

$$F(\mathbf{e}, g, \omega) = \int_{-\infty}^{\infty} \cdots \int |M(\alpha^2, \omega)|^2 \, e^{-i\boldsymbol{\alpha}\cdot\mathbf{e}} \, e^{i\omega g} e^{+i\omega\nu} \, d\nu \, d^3\mathbf{a}.$$

Window effects may be approached in another way. Consider spatial effects alone. Let $w(\mathbf{x})$ be a spatial window (units: none). Then

$$W(\boldsymbol{\kappa}) = \int_{-\infty}^{\infty} w(\mathbf{x}) \, e^{-i\boldsymbol{\kappa}\cdot\mathbf{x}} \, d^3\mathbf{x} \qquad \text{(units: m}^3\text{)}.$$

If $F(\boldsymbol{\gamma})$ is a Fourier power spectral density of an environmental disturbance, it can be "seen" through the instrumental window $w(\mathbf{x})$:

$$F(\boldsymbol{\alpha}) = \int_{-\infty}^{\infty} W(\boldsymbol{\alpha} - \boldsymbol{\gamma}) \, F(\boldsymbol{\gamma}) \, d^3\boldsymbol{\gamma}.$$

Example: Let the window be a triangle centered on x of base $2L$:

$$w(x) = 1 - \frac{|x|}{L}, \qquad |x| \leqslant L,$$

$$w(x) = 0 \qquad \text{otherwise.}$$

Then

$$W(\kappa) = \int_{-L}^{L} \left(1 - \frac{|x|}{L}\right) e^{i\kappa x} \, \frac{dx}{2\pi}$$

$$= \frac{1}{\pi} \int_0^L \left(1 - \frac{x}{L}\right) \cos\kappa x \, dx$$

$$= \frac{L}{2\pi} \left[\frac{\sin(\kappa L/2)}{\frac{\kappa L}{2}}\right]^2 \qquad \text{(units: m)}.$$

If $F(\gamma)$ is the power spectral density of a disturbance, then the convolution gives the "windowed" spectrum:

$$F(\alpha) = \frac{L}{2\pi} \int_{-\infty}^{\infty} \left[\frac{\sin\frac{L}{2}(\gamma - \alpha)}{\frac{L}{2}(\gamma - \alpha)}\right]^2 F(\gamma) \, d\gamma.$$

Now define a band of wavenumbers $\Delta\alpha$ by the requirement

$$\frac{L}{2\pi} \Delta\alpha \int_{-\infty}^{\infty} \left[\frac{\sin\frac{L}{2}\alpha}{\frac{L}{2}\alpha}\right]^2 d\left(\frac{L}{2\pi}\alpha\right) = 1.$$

The integral is equal to π. Therefore the band of wavenumbers is

$$\Delta\alpha \approx \frac{2}{L} \qquad \text{(units: m}^{-1}\text{)},$$

in which L is half of the base of the triangle representing the window. The effective band (at the 3-dB power points) is half of this. Thus,

$$\Delta\alpha_{\text{effective}} \approx \frac{1}{L}.$$

REFERENCE

B1. G.M. Corcos, "Resolution of Pressure in Turbulence," J. Acoust. Soc. Am. 35, 192 (1963).

Appendix C

FORMS OF FOURIER INTEGRALS USED IN THIS REPORT

Let $i(t)$ be a random current. Then it can be represented as a Fourier expansion,

$$i(t) = \int_{-\infty}^{\infty} e^{-i\omega t} I(\omega)\, d\omega,$$

in which $I(\omega)$ is the amplitude spectrum, with units A · s. By inverse expansion one recovers $i(t)$:

$$i(t) = \int_{-\infty}^{\infty} e^{-i\omega t} \int_{-\infty}^{\infty} i(t')\, e^{+i\omega t'}\, \frac{dt'}{2\pi}\, d\omega.$$

This is formally proved by identifying the delta function,

$$\delta(t - t') = \frac{1}{2\pi} \int_{-\infty}^{\infty} e^{i\omega(t'-t)}.$$

In this report we associate the 2π in the expansion of $i(t)$ arbitrarily with the time coordinate, i.e.,

$$I(\omega) = \int_{-\infty}^{\infty} i(t)\, e^{i\omega t'}\, \frac{dt'}{2\pi}.$$

Particularly, in the application of Rayleigh's theorem, we use the convention,

$$\frac{1}{2\pi} \int_{-\infty}^{\infty} |i(t)|^2\, dt = \int_{-\infty}^{\infty} |I(\omega)|^2\, d\omega.$$

The units of the power spectrum $|I(\omega)|^2$ are $A^2 \cdot s^2$. If the time duration of $i(t)$ is finite, say T s, then

$$\int_{-\infty}^{\infty} |i(t)|^2\, dt \;\rightarrow\; T <i^2>,$$

in which $<i^2>$ is the mean-square amplitude over T. Thus for finite signals (in time) Rayleigh's theorem has the form

$$<i^2> = 2\pi \int_{-\infty}^{\infty} \frac{|I(\omega)|^2}{T}\, d\omega,$$

in which

$$I(\omega) = \int_{-T/2}^{T/2} i(t)\, e^{i\omega t}\, \frac{dt}{2\pi}.$$

Thus,

$$\frac{2\pi |I(\omega)|^2}{T}$$

is the *power spectral density* (in units of $A^2 \cdot s$) of the random function $i(t)$ in the interval $-T/2 \leqslant t \leqslant T/2$, and $I(\omega)$ is the Fourier transform of $i(t)$.

These same conventions are applicable to spatial as well as temporal Fourier transforms. If $p(\mathbf{r}, t)$ is a random function of space and time by temperature (units: °C), then the mean-square p over all space V and time T is

$$<p^2> = (2\pi)^4 \iint \frac{|p(\mathbf{K}, \omega)|^2}{VT}\, d\mathbf{K}\, d\omega \qquad (\text{units:}(°C)^2),$$

where

$$p(\mathbf{K}, \omega) = \iint p(\mathbf{r}, t)\, e^{-i\mathbf{K}\cdot\mathbf{r}+i\omega t} \frac{dt}{2\pi} \frac{d\mathbf{r}}{(2\pi)^3} \quad (\text{units: } ℃ \cdot \text{m}^3 \cdot \text{s}).$$

Thus

$$\frac{(2\pi)^4 |p(\mathbf{K}, \omega)|^2}{VT} \qquad (\text{units: } (℃)^2 \cdot \text{m}^3 \cdot \text{s})$$

is the power spectral density of the random function $p(\mathbf{r}, t)$. Similarly, if the spatial part of the spectrum is one-dimensional, then the power spectral density is

$$(2\pi)^2 \frac{|p(\alpha, \omega)|^2}{LT} \qquad (\text{units: } (℃)^2 \cdot \text{m} \cdot \text{s}),$$

where

$$p(\alpha, \omega) = \int_{-\infty}^{\infty} p(x, t)\, e^{i\omega t - i\alpha x} \frac{dt\, dx}{(2\pi)^2} \qquad (\text{units: } ℃ \cdot \text{m} \cdot \text{s})$$

and

$$\langle p^2 \rangle = \int_{-\infty}^{\infty} (2\pi)^2 \frac{|p(\alpha, \omega)|^2}{LT}\, d\alpha\, d\omega \qquad (\text{units: } (℃)^2).$$

Appendix D

POWER SPECTRAL DENSITY FACTORS FOR sin x/x CORRELATION OF THE RANDOM FIELD

Let $i_J(t)$ be the random current caused by laser jitter. Assume that the autocorrelation function of $i_J(t)$ has a $\sin x/x$ dependency. Then

$$\Upsilon(\tau) = \langle i_J^2 \rangle \frac{\sin\pi(0.7\omega_c\tau)}{\pi(0.7\omega_c\tau)} \qquad \text{(units: A}^2\text{)}.$$

This form is selected because it closely resembles the time-delay correlograms of ambient ocean noise obtained by Urick [D1]. In addition, when $\omega_c\tau = 1$,

$$\frac{\sin\pi(0.7)}{\pi(0.7)} \approx e^{-1},$$

showing that the autocorrelation cuts off as required. Thus τ_c becomes the correlation time. Again, according to the Wiener-Kinchine theorem,

$$\frac{1}{2\pi}\int_{-\infty}^{\infty} e^{-i\omega\tau}\,\Upsilon(\tau)\,d\tau = \frac{2\pi}{T}\,|\delta S_J(\omega)|^2 \qquad \text{(units: A}^2\cdot\text{s)}.$$

Now

$$\frac{1}{2\pi}\int_{-\infty}^{\infty} e^{-i\omega\tau}\,\Upsilon(\tau)\,d\tau = \frac{B}{0.7\omega_c \times 2\pi}\int_{-\infty}^{\infty}\frac{\sin\pi x}{\pi x}\,e^{-i2\pi xs}\,dx = \frac{B}{0.7\omega_c\times 2\pi}\,\Pi\,(s),$$

where

$$x = 0.7\omega_c\tau\ ,$$

$$B = \langle i_J^2 \rangle,$$

and

$$s = \frac{\omega}{0.7\times 2\pi\omega_c}, \quad \text{and}$$

$\Pi(s)$ is the rectangular function:

$$\Pi(s) = 1 \ \text{ when } s = \frac{\omega}{0.7\times 2\pi\omega_c} < \frac{1}{2}, \text{ or } \omega < 0.7\pi\omega_c,$$

$$\Pi(s) = 0 \ \text{ when } s > \frac{1}{2}, \text{ or } \omega > 0.7\pi\omega_c.$$

Thus, the laser jitter power spectral density factor is modeled as

$$2\pi\,\frac{|\delta S_J(\omega)|^2}{T} = \frac{\langle i_J^2\rangle\,\Pi\left(\dfrac{\omega}{0.7\times 2\pi\omega_c}\right)}{0.7\omega_c\times 2\pi}$$

The autocorrelation and power spectral density factor are shown in Fig. D1.

A similar form can be obtained for one-dimensional spatial autocorrelations, viz.,

$$\Upsilon(l) = \frac{\langle i_{r,t}^2\rangle\,\sin\pi\left[0.7\dfrac{l}{lc}\right]}{\pi\left[0.7\dfrac{l}{lc}\right]} \qquad \text{(units: A}^2\text{)}.$$

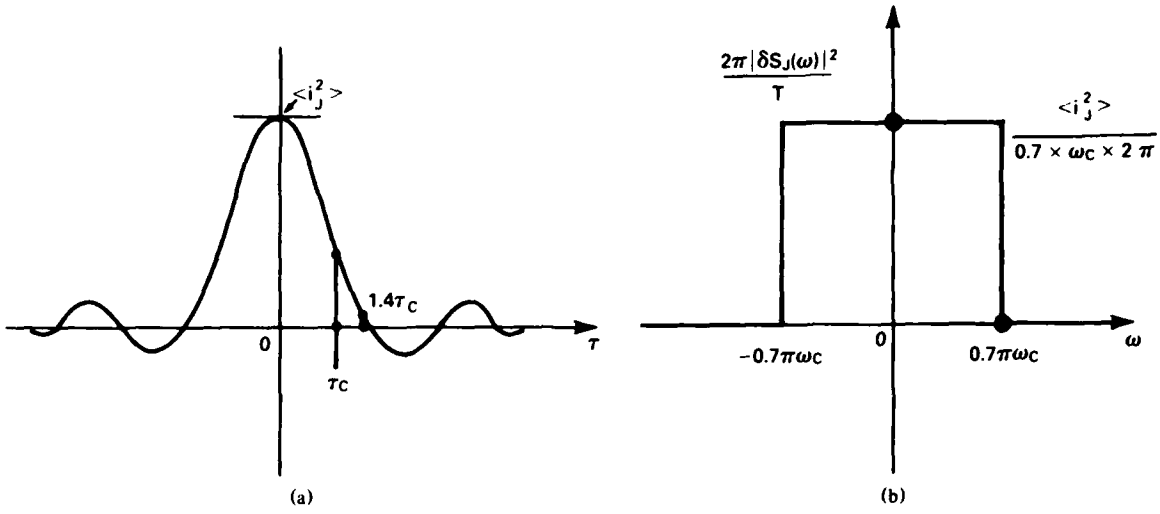

Fig. D1 — (a) Autocorrelation; (b) Power spectral density factor

The power spectral density factor over *both* space and time is, therefore,

$$(2\pi)^2 \frac{|\delta S(\alpha,\omega)|^2}{LT} = \frac{\langle i_{r,l}^2 \rangle l_c}{0.7\times 2\pi} \Pi\left(\frac{\alpha l_c}{0.7\times 2\pi}\right) \times \frac{1}{0.7\omega_c \times 2\pi} \Pi\left(\frac{\omega}{0.7\times 2\pi\,\omega_c}\right) \quad \text{(units: A}^2\cdot\text{s)},$$

in which L is the spatial interval of integration.

Summary

The noise contributions (units: A^2/Hz) from fluctuations in a laser beam and from environmental effects have been modeled on the basis of $\sin x/x$ autocorrelations. The resulting formulas for the noise are written in terms of rectangle functions $\Pi(s) = 1$, $S \leqslant 1/2$, and $\Pi(s) = 0$, $S > 1/2$

Laser beam jitter: The corresponding random photomultiplier current is $i_j(t)$, whose power spectral density factor is modeled as

$$\frac{2\pi}{T}|\delta S_J(\omega)|^2 = \frac{\langle i_J^2 \rangle}{0.7\times 2\pi\omega_{cJ}} \Pi\left(\frac{\omega}{0.7\times 2\pi\omega_{cJ}}\right) \quad \text{(units: A}^2\cdot\text{s)},$$

where ω_{cJ} is the correlation frequency.

Space- and time-varying environmental temperature: The corresponding random photomultiplier current is $i_{\delta\theta}(\mathbf{r}, t)$, whose power spectral density factor is modeled as

$$\frac{(2\pi)^2}{LT}|\delta S_{\delta\theta}(\alpha,\omega)|^2 = \frac{\langle i_{\delta\theta}^2 \rangle l_{c\theta}}{(2\pi)^2\times(0.7)^2\omega_{c\theta}} \Pi\left(\frac{\alpha l_{c\theta}}{0.7\times 2\pi}\right) \Pi\left(\frac{\omega}{0.7\times 2\pi\,\omega_{c\theta}}\right),$$

where $\omega_{c\theta}$ is the correlation frequency, and $l_{c\theta}$ is the correlation length.

3-*space and time-varying environmental mechanical stresses:* The corresponding random photomultiplier current is $i_M(\mathbf{r}, t)$, whose power spectral density factor in an isotropic environment is modeled as

$$\frac{2\pi}{VT^2}\,|\delta S_M(\mu,\omega)|^2 = \frac{\langle i_M^2\rangle\; l_{cM}^3}{(2\pi)^4\times(0.7)^4\,\omega_{cM}}\,\Pi\left(\frac{\mu\, l_{cM}}{0.7\times 2\pi}\right)\Pi\left(\frac{\omega}{0.7\times 2\pi\omega_{cM}}\right)\ \text{(units: } A^2\cdot m^3\cdot s),$$

where ω_{cM} is the correlation frequency, l_{cM} is the correlation length, and $\mu = |\boldsymbol{\mu}|$.

REFERENCE

D1. R.J. Urick, *Principles of Underwater Sound,* 1st ed., McGraw-Hill, New York, 1967, p. 187.

Appendix E

EQUIVALENT CIRCUITS OF PHOTODETECTOR AND PREAMPLIFIER

A generalized photodetector can be schematically represented as an input-signal current source i_{signal} in parallel with an admittance Y_l and a noise current source i_G. The internal current gain is $<G>$. The circuit is shown in Fig. E1.

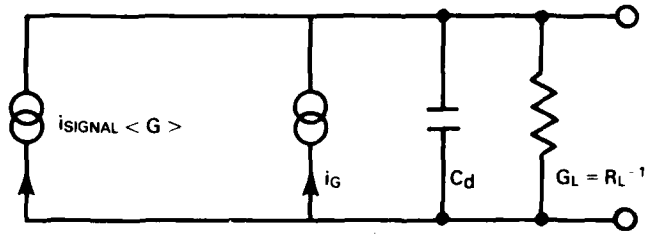

Fig. E1 — Equivalent circuit of photodetector

The noise current source is typically shot noise. Using symbols defined in the text, this noise is

$$<i_G^2> = 2e[(I_{ph})_{coh} + (I_{ph})_{incoh} + I_{BK} + I_d] <G>^2 F(G)$$

in units of A^2/Hz. It is to be noted that $i_{signal} = (I_{ph})_{coh} + (I_{ph})_{incoh}$ and that

$$Y_l = R_L^{-1} + j\omega C_d.$$

A generalized preamplifier can be schematically represented as a noiseless generator with gain $A(\omega)$ and input admittance $Y_A = G_A + j\omega C_A$. It has two noise sources [E1], a voltage noise source ν_A in series with the input terminals and an uncorrelated current noise source i_A in parallel with the input terminals. Coupled to i_A is a second current source $\nu_A Y_c$, which is correlated to ν_A through a cross admittance $Y_c = \mathrm{Re}\, Y_c + j\mathrm{Im}\, Y_c$. The equivalent circuit is shown in Fig. E2.

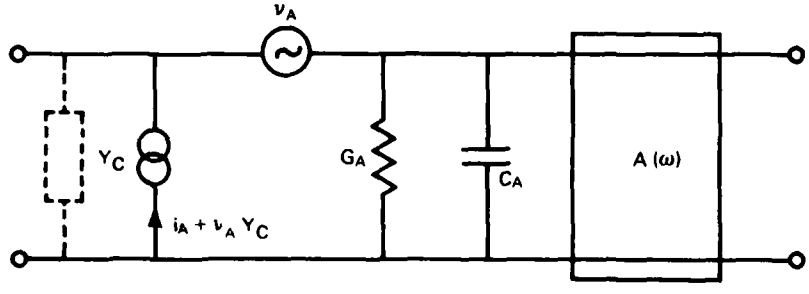

Fig. E2 — Equivalent circuit of amplifier

REFERENCE

E1. H. Rothe and W. Dahlke, "Theory of Noisy Fourpoles," Proc. IRE **44**, 811 (1956).

Appendix F

NUMERICAL CALCULATIONS OF MEAN-SQUARE PHASE FLUCTUATIONS CAUSED BY TEMPERATURE FLUCTUATIONS IN THE OCEAN

The formula derived in the text is

$$\sqrt{<\delta\phi_L^2>} = 1.40 \times 10^2 \quad \sqrt{<\delta\theta^2(\Delta\alpha, \Delta\omega)>}.$$

As noted in the section "Calculation of the Mean-Square Fluctuation in Temperature over a Towed Fiber," the mean-square temperature fluctuation for a particularly specified fiber 1000 m long at a depth of 100 m is

$$<\delta\theta^2(\Delta\alpha)> = 8.31 \times 10^{-4} \quad (°C)^2,$$

and

$$\sqrt{<\delta\phi^2>} = 1.40 \times 10^2 \times \sqrt{8.31 \times 10^{-4}} = 4.04 \text{ rad.}$$

Calculations for $L = 100$ m, 10 m, and 1 m are shown below.

$L = 100$ m, $\hat{\alpha}_{1_{min}} = 10^{-2}$ cpm:

$$I = (1.22 \times 10^{-4})^2 \times \frac{1}{10^{-2}} = 1.4884 \times 10^{-6},$$

$$\int \hat{F}_\zeta(\alpha_1)\, d\hat{\alpha}_1 = 8.925 \times 10^4 \times 1.4884 \times 10^{-6}$$

$$= 1.33 \times 10^{-1} \text{ m}^2,$$

$$<\delta\theta^2> = (0.025)^2 \times 1.33 \times 10^{-1} = 8.31 \times 10^{-5} \quad (°C)^2,$$

and

$$\Delta\phi = 1.40 \times 10^2 \times \sqrt{8.31 \times 10^{-5}} = 1.28 \text{ rad.}$$

$L = 10$ m, $\hat{\alpha}_{1_{min}} = 10^{-1}$ cpm:

$$I = (1.22 \times 10^{-4})^2 \frac{1}{10^{-1}} = 1.4884 \times 10^{-7},$$

$$\int \hat{F}_\zeta(\alpha_1)\, d\hat{\alpha}_1 = 8.925 \times 10^4 \times 1.4884 \times 10^{-7}$$

$$= 1.33 \times 10^{-2} \text{ m}^2,$$

$$<\delta\theta^2> = (0.025)^2 \times 1.33 \times 10^{-2} = 8.31 \times 10^{-6},$$

and

$$\Delta\phi = 1.40 \times 10^2 \times \sqrt{8.31 \times 10^{-6}} = 0.404 \text{ rad.}$$

$L = 1$ m, $\hat{\alpha}_{1_{min}} = 1$ cpm:

$$I = (1.22 \times 10^{-4})^2 \times \frac{1}{1} = 1.4884 \times 10^{-8},$$

$$\int \hat{F}_\zeta(\alpha_1)\, d\hat{\alpha}_1 = 8.925 \times 10^4 \times 1.4884 \times 10^{-8}$$
$$= 1.33 \times 10^{-3},$$
$$\langle \delta\theta^2 \rangle = (0.025)^2 \times 1.33 \times 10^{-3} = 8.31 \times 10^{-7},$$

and

$$\Delta\phi = 1.40 \times 10^2 \times \sqrt{8.31 \times 10^{-7}} = 0.128 \text{ rad.}$$

These results are listed in Table 2 in the text.

Appendix G

STRUCTURE FUNCTIONS OF TEMPERATURE AND LIEBERMANN'S MODEL

Let $C(x, t)$ be the speed of sound at point x in the ocean. Assume that the ocean is "frozen" temporarily and plot $C(x)$ vs x. It is found that $C(x)$ is a random function with mean $C_0(x)$ and a fluctuation. Suppose that the mean value is subtracted out, and designate the remaining fluctuating part by $\delta C(x)$. Now at point x one can find $\delta C^2(x)$. The ensemble average of $\delta C^2(x)$ for all x is its *variance*. The square root of the variance is the standard deviation of $C(x)$ at x, i.e.,

$$\sigma(x) = \sqrt{<C^2(x)>}.$$

Between *two* points, x and $x + \rho$, there will be a finite difference in $C(x)$. By selecting a large number of two-point pairs, one can construct the ensemble average, or *structure function*, $D_c(\rho)$,

$$D_c(\rho) = <[\delta C(x+\rho) - \delta C(x)]^2> = <\delta C^2(x+\rho)> + <\delta C^2(x)> - 2<\delta C(x+\rho\delta C(x)>.$$

Assume that $\delta C(x)$ is statistically stationary in space, then

$$<\delta C^2(x)> = <\delta C^2(x+\rho)> = <\delta C^2(0)>.$$

Therefore,

$$D_c(\rho) = 2[R_c(0) - R_c(\rho)],$$

in which

$$R_c(\rho) = <\delta C(x+\rho)\delta C(x)>,$$

i.e., $R_c(\rho)$ is the autocorrelation of the zero mean fluctuation. Dividing through by $R_c(0)$, one has

$$\frac{<[\delta C(x+\rho) - \delta C(x)]^2>}{<\delta C^2(0)>} = 2\left[1 - \frac{R_c(\rho)}{R_c(0)}\right].$$

This is the average difference squared between two points of the frozen fluctuation pattern normalized to the variance at a point. Since

$$C(x+\rho) - C(x) = C_0(x+\rho) + \delta C(x+\rho) - C_0(x) - \delta C(x),$$

we can say that, for a short distance, $C_0(x+\rho) - C_0(x) \approx 0$. Hence, we can say that $\delta C(x+\rho) - \delta C(x)$ measures the spatial gradient of the speed of sound.

The speed of sound is a function of temperature, salinity, pressure, etc. In the first approximation, for temperature $\mathcal{T}$(°C), assume

$$C(x) = C_0 + 421\,\mathcal{T}(x) + \ldots \quad \text{(units: cm/s)}.$$

Thus, if $\delta T(x)$ is the *zero-mean fluctuation* of $\mathcal{T}$, then $\Delta C(x) = 421\,\delta T(x)$ and

$$C(x+\rho) - C(x) \approx 421[\delta T(x+\rho) - \delta T(x)].$$

Since we are normalizing with respect to the variance of the fluctuation in $C(x)$ at a point, we see that

$$\frac{<[\delta T(x+\rho) - \delta T(x)]^2>}{<\delta T^2(0)>} = 2\left[1 - \frac{R_T(\rho)}{R_T(0)}\right].$$

Liebermann [G1] measured temperature fluctuations in the ocean at depths of 30 to 60 m. He found that the mean temperature fluctuation at a point averaged over his record was about 0.04°C and

that the correlation length in *temperature fluctuation* between points was about 60 cm. The mean-square fluctuation in *index of refraction* was 5×10^{-9}. Thus, between any two points along a track at these depths the ensemble-averaged difference in temperature, i.e., difference in fluctuation of temperature (assuming the mean is subtracted out), is

$$<[\delta T(x+\rho) - \delta T(x)]^2> = <\delta T^2(\rho)> = 2 \times 0.04^2 [1 - R_T(\rho)],$$

in which $R_T(\rho)$ is the normalized autocorrelation of the zero-mean function $\delta T(x)$.

Now Liebermann also found that the normalized autocorrelation in $C(x)$ can be modeled as

$$R(\rho) = \frac{30}{29} e^{-\frac{\rho}{60}} - \frac{1}{29} e^{-\frac{1}{2}\rho}, \quad \rho = \text{separation distance of points.}$$

Hence the horizontal temperature gradients in the ocean due to fluctuations (with mean values subtracted out) are given by

$$\sqrt{<\Delta T^2(\rho)>} = \sqrt{2} \times 0.04 \left[1 - \frac{30}{29} e^{-\frac{\rho}{60}} + \frac{1}{29} e^{-\frac{\rho}{2}}\right]^{1/2} \quad \text{(units: °C)}.$$

Temperature gradients based on this formula are given in Table G1.

Table G1 — Temperature Gradients

ρ (cm)	$1 - R(\rho)$	$\sqrt{<\Delta T^2(\rho)>}$ (°C)
0.1	4.0957×10^{-5}	3.62×10^{-4}
1.0	3.53058×10^{-3}	3.36×10^{-3}
40	4.6887×10^{-1}	3.87×10^{-2}
60	6.194×10^{-1}	4.45×10^{-2}
∞	1	5.66×10^{-2}

REFERENCE

G1. L. Liebermann, "The Effect of Temperature Inhomogeneities in the Ocean on the Propagation of Sound," J. Acoust. Soc. Am. **23**, 563 (1951).

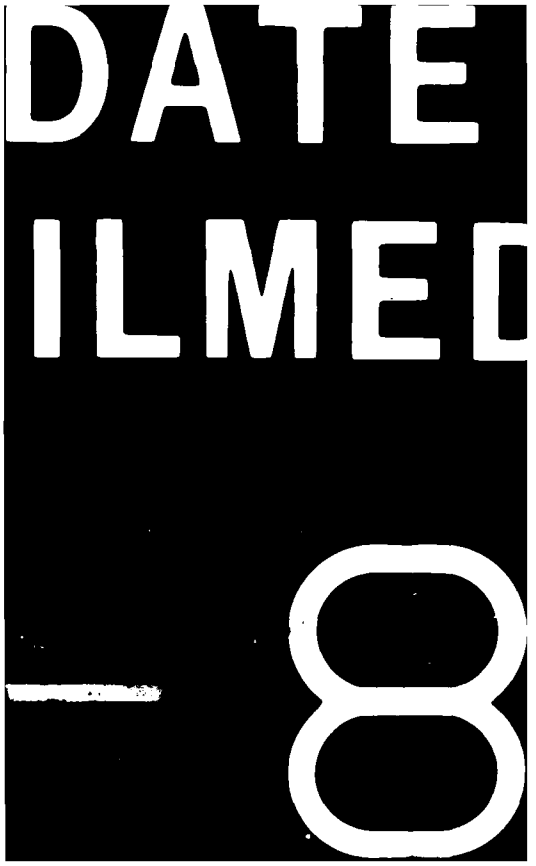
DATE
ILMED
8